ELSEVIER

Coordination Chemistry Reviews
214 (2001) 1–42

COORDINATION CHEMISTRY REVIEWS

www.elsevier.com/locate/ccr

Annual survey of organometallic metal cluster chemistry for the year 1999

Michael G. Richmond *

Department of Chemistry, University of North Texas, Denton, TX 76203, USA

Received 7 November 2000; accepted 9 November 2000

Contents

Abstract

The synthetic, mechanistic, and structural chemistry of organometallic metal cluster compounds is reviewed for the year 1999.

Keywords: Organometallic metal cluster compounds; Synthetic; Mechanistic

* Tel.: + 1-817-5653548; fax: 1-940-5654318.

0010-8545/01/$ - see front matter
PII: S0010-8545(00)00400-8

1. Dissertations

The vanadium cluster $[Cp^*V(\mu_2\text{-}Cl)_2]_3$ has been synthesized from $VCl_3(THF)_3$ and Cp^*SnBu_3. The metallic core of this cluster consists of an equilateral triangle with each edge of the triangle being bridged by two chlorine atoms. Complicated antiferromagnetic behavior was observed over the temperature range 2–300 K. Treatment of this cluster with NaN_3 affords $[Cp^*V(\mu_2\text{-}N)Cl]_2$, which when allowed to react with strong reducing agents gives the tetravanadium cluster $[Cp^*V(\mu_3\text{-}N)]_4$. X-ray diffraction analysis confirms the cubane geometry present in this V_4 cluster [1]. Rapid intramolecular electron transfer has been verified in the ligand-bridged clusters $Ru_3(\mu_3\text{-}O)(\mu\text{-}OAc)_6(CO)(L')(\mu\text{-}L)Ru_3(\mu_3\text{-}O)(\mu\text{-}OAc)_6(L'')$. The magnitude of the electronic coupling (H_{AB}) has been estimated to be on the order of 6050 cm^{-1} to 1310 cm^{-1}. Trends as a function of the bridging L′ ligand are discussed [2]. The synthesis and reactivity of new acetylide- and SO_2-containing clusters have been published. Part of these reactivity studies has concentrated on the transformations available to the ancillary CO ligands. Treatment of $[PPN]_2[Fe_3(CO)_9(CCO)]$ with a McMurry coupling reagent yields the new clusters $[PPN][Fe_3(CO)_9(CCH)]$ and $Fe_3(CO)_9[CCOTi(THF)_4Cl]$, in addition to the known cluster $Fe_3(CO)_{10}(CCH_2)$. The reaction of SO_2 with the heterometallic clusters $[PPN]_2[MFe_3(CO)_{13}]$ (where M = Cr, W) produces a variety of SO_2 and sulfide clusters. The reactivity of $[PPN]_2[Ru_3(CO)_9(\mu_3,\eta^2\text{-}SO_2)]$, $[PPN][HRu_3(CO)_8(\mu\text{-}SO_2)(\mu_3,\eta^2\text{-}SO_2)]$, and $[PPN][Ru_3(CO)_7(\mu\text{-}SO_2)_2(\mu_3,\eta^2\text{-}SO_2)]$ with several different electrophiles has also been examined, with characterization directed at the site of alkylation [3]. Methodology for the functionalization of heterocycles using electron-deficient bonding to triosmium clusters is presented. The carbocyclic ring of quinolines is readily substituted by incoming nucleophiles due to the electron-deficient bonding of the C(8) carbon center and protective coordination of the nitrogen atom. Mechanistic details, spectroscopic data, and X-ray crystallographic results are fully discussed [4]. Oxidation of tetracyanoplatinates affords numerous species, one of which has been characterized as $[Pt_3(CN)_8]^{3-}$ by ^{195}Pt-NMR spectroscopy [5].

Details on the functionalization of cyclopentadienyl ligands in $Cp_4Fe_4(CO)_4$ are discussed. Thermolysis of this cluster in xylene in the presence of PPh_3 affords $(C_5H_4Ph)Cp_3Fe_4(CO)_4$ and $Cp_3Fe_3(CO)_3(PPh_2)$. Cp ring alkylation in $Cp_4Fe_4(CO)_4$ is also achieved by using LDA, followed by treatment with electrophiles. Di- and trifunctionalized derivatives are possible under these conditions. The X-ray structures of $[(C_5H_4)Cp_3Fe_4(CO)_4]_2CHOH$ and $(C_5H_4PPh_2)Cp_3Fe_4(CO)_4RuCl_2$(cymene) are included in this dissertation [6]. New rhodium/gold and iridium/gold oxo-containing clusters have been prepared. These clusters are obtained from the reaction between $[(AuPPh_3)_3(\mu\text{-}O)][BF_4]$ and $[M(diene)Cl]_2$. Also presented are the syntheses and structural properties of the platinum/gold complexes $[(1,5\text{-}COD)Pt(\mu\text{-}OAuL)]_2[BF_4]_2$ (where L = various phosphines) and the gold-free cluster $[(1,5\text{-}COD)_4Pt_4(\mu_3\text{-}O)_2(\mu\text{-}OH)][BF_4]_3$ [7].

The coordination chemistry and reactivity of polythioether macrocycles at ruthenium clusters have been examined. Two of the clusters employed were

$Ru_5(CO)_{15}(\mu_5\text{-C})$ and $Ru_6(CO)_{17}(\mu_6\text{-C})$. A new catalytic route to polyselenoether macrocycles has been discovered, and the details associated with the catalytic cyclooligomerization of 3,3-dimethylselenatane are presented [8]. The two-electron redox chemistry of $Fe_3(CO)_9[\mu_3\text{-}PMn(CO)_2Cp]_2$ is discussed with respect to iron-iron bond cleavage and reformation. The utility of the dianion in small molecule coupling reactions is presented. A method has been developed in order to determine the protonation rate of cluster dianions by using cyclic voltammetric analysis in the pseudo first-order kinetic regime. The X-ray crystal structures of five clusters are reported [9].

The synthesis and reactivity of several hexaplatinum clusters stabilized by the diphosphine ligand dppm are described. Reversible oxidation of the 84-electron cluster $Pt_6(\mu_2\text{-}CO)_6(\mu_2\text{-dppm})_3$ affords the corresponding 82-electron cluster, which exhibits a distorted octahedral Pt_6 core, as revealed by X-ray diffraction analysis. Treatment of $Pt_6(\mu_2\text{-}CO)_6(\mu_2\text{-dppm})_3$ with $[M(CO)_4]^-$ (where M = Rh, Ir) affords the monocapped heteronuclear clusters $[Pt_6\{\mu_3\text{-}M(CO)_2\}(\mu_2\text{-}CO)_6(\mu_2\text{-dppm})_3]^-$. The nature of the observed products reveals that unique cooperation exists between the two Pt_3 faces in the starting Pt_6 cluster, manifesting itself in one Pt_3 face directing the substitution reaction relative to the other Pt_3 face. Acetylene ligands are shown to oxidatively degrade $Pt_6(\mu_2\text{-}CO)_6(\mu_2\text{-dppm})_3$ to yield the platinum dimer $Pt_2(CO)_2(\mu_2\text{-RCCR})(\mu_2\text{-dppm})$ as the only dppm-containing product [10]. A dissertation describing the syntheses and X-ray structural analyses of new high-nuclearity homometallic/heterometallic palladium and gold/nickel clusters has been published. Some of the clusters discussed include $Pd_{16}(CO)_{13}(PMe_3)_9$, $Pd_{35}(CO)_{23}(PMe_3)_{15}$, $Pd_{39}(CO)_{23}(PMe_3)_{16}$, $Pd_{59}(CO)_{32}(PMe_3)_{21}$, and $Pd_{29}Ni_3(CO)_{22}(PMe_3)_{13}$. The Pd_{59} cluster is the largest crystallographically determined discrete metal cluster with direct M–M bonding reported to date [11].

2. Homometallic clusters

2.1. Group 5 clusters

The reductive aggregation of $Cp^*VCl_2(O)$ using strong reducing agents (sodium, potassium, magnesium, calcium) gives the cubane-like cluster $[Cp^*V(\mu_3\text{-}O)]_4$ and the adamantane-like cluster $(Cp^*V)_4(\mu\text{-}O)_6$. A mechanistic scheme accounting for the formation of these clusters is presented, and the details associated with the observed magnetic behavior of these two clusters are discussed. The X-ray structure of the latter product cluster is presented [12].

2.2. Group 6 clusters

$[CpCr(CO)_3]_2$ reacts with Sb_2S_3 under mild conditions to furnish $[CpCr(CO)_2]_2S$ and $[CpCr(CO)_3]_4(Sb_2S)$. The molecular structure of the Cr_4 product exhibits a 'bare' antimony-sulfur bridging ligand [13]. The reaction between $[CpCr(CO)_3]_2$ and P_4Se_3 gives $Cp_4Cr_4(CO)_8(P_2Se_2)$, along with several mono- and dinuclear by-prod-

ucts. The Cr_4 compound has been characterized in solution and by X-ray crystallography, which has revealed an unusual open-book framework with a P–P bond as its backbone [14]. New heterometallic cubane-like clusters having the general formula $[(CpMo)_3S_4\{M(CO)_3\}](p$-toluenesulfonate) (where M = Mo, W) have been synthesized and thoroughly characterized in solution. The X-ray structure of the Mo_3W derivative consists of a heterometallic S_4-capped tetrahedral core [15]. Treatment of $CrCl_3(THF)_3$ with $Li(CH_2CH_2CH_2NMe_2)$ in THF at room temperature (r.t.) yields the tetranuclear complex $Cr_4(CH_2CH_2CH_2NMe_2)_4(\mu_4\text{-}O)(\mu\text{-}Cl)_6$. The molecular structure reveals that each chromium center possesses a distorted octahedral coordination geometry [16]. New structural motifs in metalloborane chemistry have been elucidated by using *nido* 2-$Cp^*H_3WB_4H_8$ as a starting material. Pyrolysis of *nido* 2-$Cp^*H_3WB_4H_8$ gives the unsaturated, reactive species $Cp^*HWB_4H_8$, which ultimately affords the complexes $(Cp^*W)_2B_2H_9$, $(Cp^*W)_3(\mu\text{-}H)B_8H_8$, and $(Cp^*W)_2B_7H_9$. The tritungsten cluster has been structurally characterized (Fig. 1) and is shown to be analogous to a known Ru_{11} cluster consisting of a hexagonal close packed metal core. This closed, boron-rich metalloborane cluster is best described as a $(n-4)$ SEP system. Fenske–Hall MO calculations confirm the observed polyhedral shape found in $(Cp^*W)_3(\mu\text{-}H)B_8H_9$ [17].

2.3. Group 7 clusters

The cluster $[Mn_4(CO)_{12}(\mu_4\text{-}Te)_2][PPN]_2$ has been synthesized from $Mn_2(CO)_{10}$ and K_2TeO_3 in MeOH. Methylation of this cluster with $MeSO_3CF_3$ affords the pentamanganese cluster $[(TeMe_2)Mn(CO)_5(\mu_5\text{-}Te)Mn_4(CO)_{12}][PPN]$. Both clusters represent the first examples of tellurido-manganese carbonyl clusters that contain four

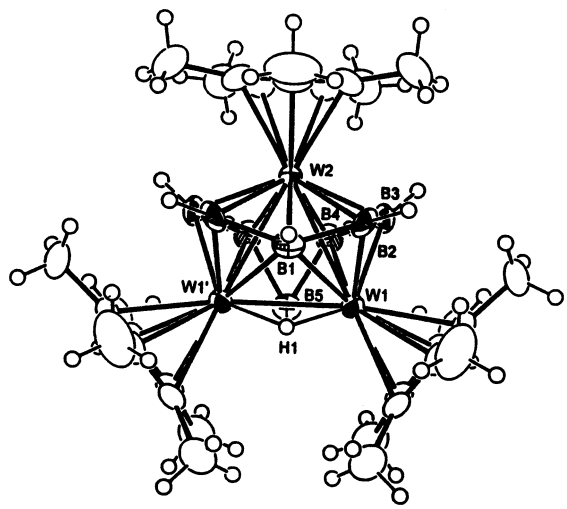

Fig. 1. X-Ray structure of $(Cp^*W)_3(\mu\text{-}H)B_8H_8$. Reprinted with permission from Organometallics. Copyright 1999 American Chemical Society.

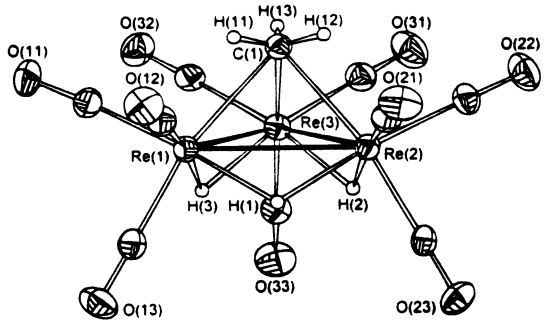

Fig. 2. X-Ray structure of $[Re_3(\mu\text{-}H)_3(\mu_3\text{-}CH_3)(CO)_9]^-$. Reprinted with permission from Journal of American Chemical Society. Copyright 1999 American Chemical Society.

manganese–manganese bonds. The solution spectroscopic data and X-ray crystallographic results are discussed [18]. A high-yield and simple synthesis of $Re_3(\mu\text{-}H)_3(CO)_{12}$ starting from $Re_2(CO)_{10}$ has been published. This new method employs the hydrogenation of $Re_2(CO)_{10}$ under solvothermal reaction conditions [19]. The synthesis of $[HRe_4(CO)_{17}]^-$ from $Re_2(CO)_{10}$ and a samarium pyrazolylborate reducing agent has been reported. This 64-electron Re_4 cluster adopts a spiked triangular structure with the hydride ligand bridging two rhenium atoms in the equatorial plane [20]. A report on the synthesis of the first rhenium carbonyl cluster containing a cyclohexane-like structure has appeared. The novel Re_6 cluster, $[Re_6(\mu\text{-}H)_5(CO)_{24}]^-$, is obtained from the reaction of $[Re_4H_2(\mu\text{-}H)_3(CO)_{16}]^-$ with $Re_2(CO)_8(THF)_2$. X-ray diffraction analysis has verified the unprecedented cyclohexane-like geometry for this 96-valence electron species, and it is the first example of a hexagonal frame of metal centers built from three-center, two-electron M–H–M bonds and two-center, two-electron M-M bonds [21]. A Re_3 cluster containing a μ_3-CH_3 unit has been synthesized and structurally characterized. Treatment of $[Re_3(\mu\text{-}H)_3(\mu_3\text{-}H)(CO)_9]^-$ with ethereal diazomethane produces an almost quantitative yield of $[Re_3(\mu\text{-}H)_3(\mu_3\text{-}CH_3)(CO)_9]^-$. The nearly equilateral rhenium atom triangle is capped by a triply bridging methyl ligand (Fig. 2). ^{1}H-NMR studies dealing with the different possible isotopomers of the methyl group, coupled with ^{1}H-NMR relaxation measurements, support a solution structure having C_{3v} symmetry [22].

2.4. Group 8 clusters

The clusters $M_3(CO)_{12}$, $H_4M_4(CO)_{12}$, $[H_3M_4(CO)_{12}]^-$ (where M = Ru, Os), and $[Ru_6C(CO)_{16}]^{2-}$ have been prepared in high yields via a one-pot controlled reduction of MCl_3 or $[M(CO)_3(Cl)_2]_2$. These reactions occur under mild reaction conditions requiring atmospheric pressures of CO and alkali carbonates. The reaction parameters are discussed, and it is shown that these syntheses are more convenient than those previously reported in solution or on a silica surface [23]. $RuO_2{\cdot}xH_2O$ has been allowed to react with CO (5–20 atm) to afford $Ru_3(CO)_{12}$ in

excellent yield. When the same reaction is carried out in formic or acetic acid, the ruthenium carboxylate complexes $[Ru_2(CO)_4(O_2CR)_2]_n$ are obtained in almost quantitative yield. The use of these compounds in the reductive carbonylation of nitrobenzene in aniline furnishes *N*,*N*′-diphenylurea [24]. The X-ray structure of $[Ru_3(CO)_{11}]^{2-}$ has been determined. A single bridging CO group spanning one Ru–Ru vector was found, in agreement with the IR and ^{13}C-NMR data [25]. The results of VT X-ray diffraction studies on $Fe_nRu_{3-n}(CO)_{12}$ (where $n = 1, 2$) and the low-temperature phase of $Fe_3(CO)_{12}$ have been published. The metal atom disorder in the two mixed-metal clusters has been shown to be dynamic in origin. $Fe_3(CO)_{12}$ undergoes a phase transition at ca. 210 K to a second monoclinic phase that has a partial ordering of the Fe_3 triangles. The structural changes are discussed relative to the published fluxional mechanisms in $M_3(CO)_{12}$ clusters [26].

A report describing the catalytic carbonylation of ammonia using $Ru_3(CO)_{12}$ as the catalyst precursor has appeared. The urea product is produced under mild temperature and gas pressures [27]. Sequential insertion of CO and ethylene into C–H bonds of 1-azadienes produces 1,3-dihydropyrrol-2-one derivatives in moderate to excellent yields. $Ru_3(CO)_{12}$ catalyzes this reaction, where two new C–C bonds and a new center of asymmetry at C-3 are created [28]. $Ru_3(CO)_{12}$ functions as a catalyst for the conversion of yne-imines and CO to bicyclic α,β-unsaturated lactams. Plausible schemes and the effect of substrate substituents on these reactions are discussed [29]. The first catalytic carbonylative [4 + 1] cycloaddition using a 1,3-conjugated substrate has been published. Use of $Ru_3(CO)_{12}$ as a catalyst in this reaction promotes the transformation of α,β-unsaturated imines to unsaturated γ-lactams in the presence of CO. A working catalytic mechanism is presented [30]. The $Ru_3(CO)_{12}$-catalyzed decarbonylative cleavage of a C–C bond in alkyl phenyl ketones is described. An important feature in this report is the chelation of a substrate nitrogen to a ruthenium atom, which assists in the formation of a metallocycle during the cleavage of the C–C bond [31]. A report describing the catalytic C–H bond/alkene coupling directed by *N*,*O*-heterocyclic substituents has appeared. Use of $Ru_3(CO)_{12}$ and triethoxyvinylsilane allows for the functionalization of the C–H bond that is α to the heterocyclic atom [32]. The cyclization of 6-aminohex-1-yne to 2-methyl-1,2-dehydropiperidine by $Ru_3(CO)_{12}$ is reported [33]. A report on the hydroformylation of styrene using $Ru_3(CO)_{12}$/1,10-phen (and other nitrogen ligands) has appeared. The ratio of branched-to-linear aldehydes is discussed. Whereas the hydroformylation of methyl acrylate using $Ru_3(CO)_{12}$/1,10-phen affords 4-methoxy-4-methyl-δ-valerolactone, use of $Ru_3(CO)_{12}/PPh_3$ as the catalyst furnishes the open-chain aldehyde dimethyl 2-formyl-2-methylglutarate, which is the precursor for the above δ-lactone [34]. The mechanism of the $Ru_3(CO)_{12}/R_4NX$ catalyzed carbonylation of nitroarenes to carbamates has been explored. A revised catalytic picture is presented, which shows the carbonylation reaction proceeding through the intermediate formation of aniline and a mononuclear catalytic species. It is shown that the effect of chloride is to accelerate the formation of $Ru(CO)_5$. A detailed reaction picture is presented and fully discussed [35]. The catalytic allylic amination of an unactivated alkene using $Ru_3(CO)_{12}$/Ar-BIAN is described. The nitrogen source in these reactions is a nitroarene. Kinetic data, substituent effects, and working catalytic schemes are discussed [36].

The reaction of β-styrylpentamethyldisilane with $Ru_3(CO)_{12}$ leads to β-styryltrimethylsilane, along with the elimination of one dimethylsilylene unit. Catalytic schemes involving silapropenyl and silylene ruthenium complexes as key intermediates are presented [37]. Dehydrogenative coupling reactions of bis(hydrosilyl)benzenes with $Ru_3(CO)_{12}$ produce the polymers $[–SiRR'–Ru(CO)_4–Ru(CO)_4–SiRR'–C_6H_4–]_n$, which exhibit large solvent-dependent UV-vis spectral changes. The absorption maximum found in each of these polymers is considerably red-shifted relative to the monomeric complex $PhMe_2SiRu(CO)_4Ru(CO)_4SiMe_2Ph$. The UV-vis data of the polymers and the X-ray structure of the monomeric Ru_2 complex are discussed [38]. Regioselective alkane activation by $(Cp^*Ru)_3(\mu\text{-}H)_3(\mu_3\text{-}H)_2$ has been demonstrated [39].

A review describing the effects of halides and related ligands on the reactions of carbonylruthenium complexes has been published [40]. The reactivity of $[Ru_2(CO)_4Cl_5]^-$ under a variety of conditions has been investigated. $Ru_3(CO)_{12}$ may be synthesized from this Ru_2 complex under CO and KOH [41]. A study presenting a practical synthesis of aromatic ketimines through the use of $Ru_3(CO)_{12}$ catalysis has appeared. Here a terminal alkyne and a primary amine may be coupled to furnish the aromatic ketimine product. The utility of this hydroamination reaction is demonstrated by the two-component synthesis of quinolines [42]. Treatment of $Ru(CO)_3Cl_2(THF)$ with KOH and CO under selective reaction conditions gives the clusters $Ru_3(CO)_{12}$, $[Ru_8(\mu\text{-}CO_3)_4(\mu\text{-}Cl)_4(CO)_{16}]^{3-}$, and $[Ru_4(\mu\text{-}O)(\mu\text{-}Cl)_4(CO)_{10}]^{2-}$ [43].

Reduction of $[PPN]_2[Fe_3(CO)_9(CCO)]$ with either $TiCl_3(DME)_{1.5}$ or Zn/Cu couple affords the new cluster $[PPN][Fe_3(CO)_9(C{\equiv}CH)]$ as the major product, along with minor amounts of the known cluster $Fe_3(CO)_9(CCH_2)$ and the new cluster $Fe_3(CO)_9[CCOTi(THF)_4Cl]$. Both new products were fully characterized in solution by IR and ^{13}C-NMR spectroscopy, and by X-ray diffraction analysis (Fig. 3) [44].

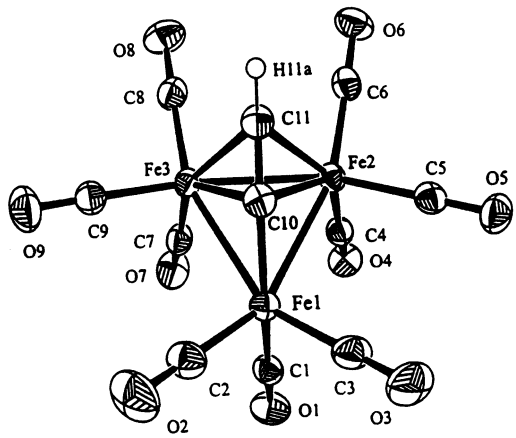

Fig. 3. X-Ray structure of $[PPN][Fe_3(CO)_9(C{\equiv}CH)]$. Reprinted with permission from Organometallics. Copyright 1999 American Chemical Society.

The cluster complex $[Fe_2Sb(CO)_5Cp]_4$ has been obtained from the thermolysis of $[\{Fe(CO)_4\}_2\{CpFe(CO)_2\}SbI]^-$. The X-ray structure reveals the existence of a cubane core, where each Sb atom serves as a μ_4-ligand between three iron atoms and one terminal $CpFe(CO)_2$ group [45]. Thermolysis of $Fe_2(CO)_6(\mu\text{-}PPh_2)(\mu\text{-}C_2^tBu)$ furnishes the dinuclear alkenyl complex $Fe_2(CO)_5(\mu\text{-}PPh_2)(\mu\text{-}o\text{-}Ph_2PC_6H_4C{=}CH^tBu)$ and the triiron cluster $Fe_3(CO)_4(\mu_3\text{-}o\text{-}PhPC_6H_4PPh)[\mu_3\text{-}C(^tBu)CCH{=}C^tBu\text{-}\mu_6\text{-}C_6H_5]$. The X-ray structure of the Fe_3 cluster has one face capped by an *ortho*-phenylenebis(phenylphosphido) ligand and a second face ligated by the enyne ligand 2,2,7,7-tetramethyl-3-phenylocta-3-en-5-yne, as confirmed by X-ray crystallography [46]. The reaction between $Ru_3(CO)_{12}$ and $dppmSe_2$ produces the open-triangular *nido* cluster $Ru_3(CO)_7(\mu_3\text{-}Se)_2(\mu\text{-}dppm)$, the *closo*-octahedral cluster $Ru_4(CO)_8(\mu\text{-}CO)(\mu_4\text{-}Se)_4(\mu\text{-}dppm)$, and the cubane-like complex $Ru_4(CO)_{10}(\mu_3\text{-}Se)_4(\mu\text{-}dppm)$. VT-NMR data on the Ru_3 cluster support fluxional behavior arising from the reversible migration of a Ru–Ru bond and an oscillation of the methylene group of the dppm ligand. Pyrolysis of the Ru_3 product cluster gives the condensation product $Ru_6(CO)_{12}(\mu_3\text{-}Se)_4(\mu\text{-}dppm)_4$, which is shown by X-ray analysis to contain a central 64-electron butterfly core [47]. A report on the chelating versus bridging behavior and NMR fluxionality of the dppf ligand in $M_3(CO)_7(\mu_3\text{-}Se)_2(dppf)$ (where M = Fe, Ru) has been published. These products are obtained from the reaction between $M_3(CO)_{12}$ and $dppfSe_2$ using Me_3NO activation. The X-ray structure of the Ru_3 cluster is included [48]. The synthesis of sulfur-capped clusters having bridging phosphido groups has been achieved by using the reagent $Ph_2P(SCMe_3)$. Treatment of $Fe(CO)_5$ with $Ph_2P(SCMe_3)$ at elevated temperature and pressure gives $Fe_3(CO)_6(\mu\text{-}CO)(\mu_3\text{-}S)(\mu\text{-}PPh_2)_2$ as the major product, along with minor amounts of $Fe_4(CO)_{12}(\mu\text{-}PPh_2)_2(\mu_4\text{-}S_2)$. The reactivity of the triiron cluster with phosphines, phosphites, and terminal alkyne ligands is presented. Four X-ray structures accompany this report [49]. The clusters $Ru_3(CO)_9L_3$ [where L = $PPh_n(C_6H_4OMe\text{-}p)_{3-n}$, $PPh_n(C_6H_4NMe_2\text{-}p)_{3-n}$ ($n = 0$–3), and $As(C_6H_4OMe\text{-}p)_3$] have been studied by electrospray mass spectrometry. The utility of these 'electrospray-friendly' ligands in cluster identification is discussed [50]. The new trifluoromethyl-phosphinidene and -arsinidene capped clusters $Ru_3(CO)_9(\mu\text{-}H)_2(\mu_3\text{-}PCF_3)$, $Ru_4(CO)_{13}(\mu\text{-}H)_2(\mu_4\text{-}PCF_3)$, $Ru_4(CO)_{12}(\mu\text{-}H)_2(\mu_3\text{-}ECF_3)_2$ (where E = P, As), $Ru_5(CO)_{15}(\mu\text{-}H)_2(\mu_3\text{-}PCF_3)_3$, $Ru_5(CO)_{15}(\mu_4\text{-}PCF_3)$, $Ru_4(CO)_{13}(\mu\text{-}H)_2(\mu_3\text{-}AsCF_3)$, $Ru_4(CO)_{13}(\mu_3\text{-}AsCF_3)_2$, and $Ru_5(CO)_{15}(\mu\text{-}H)_2(\mu_3\text{-}AsCF_3)_3$ have been isolated from the reaction between $Ru_3(CO)_{12}$ and CF_3EH_2. Two X-ray structures have been determined, and the fluxional behavior of these clusters has been investigated by VT ^{1}H-NMR spectroscopy [51]. The reaction of $Ru_3(CO)_{12}$ with $(CF_3)_2EH$ (where E = P, As) has been explored, and the molecular structures of $Ru_3(CO)_8(\mu\text{-}H)_2[\mu\text{-}P(CF_3)_2]_2$ and $[Ru_3(CO)_{10}(\mu\text{-}H)]_2[\mu\text{-}P(CF_3)_2]_2$ determined by X-ray diffraction methods [52].

The water-soluble ruthenium clusters $Ru_3(CO)_{12-x}(TPPTS)_x$ (where $x = 1$–3) and $H_4Ru_4(CO)_{11}(TPPTS)$ have been employed as catalyst precursors in the hydrogenation of non-activated alkenes under biphasic conditions. The reported catalytic turnovers are up to ca. 500 ($mol^{-1}\ h^{-1}$). The use of ionic liquid-organic and silica supports are less effective than the aqueous-organic reaction medium [53]. The

cluster $Ru_3(CO)_{10}$(dppm) isomerizes 1-hexene to the kinetic product *cis*-2-hexene at low H_2 pressure. The reaction kinetics have been investigated, and turnover frequency data support the involvement of cluster catalysis [54]. An identical study, with comparable results, has been carried out by using the cluster $Ru_3(CO)_8(dppm)_2$ as the catalyst precursor by the same researchers [55]. The reaction between $Ru_3(CO)_{10}$(μ-dppm) and $[Ru(CO)_2(\eta\text{-}C_5H_4R)]_2$(μ-C≡C) has been reexamined. Besides the originally reported products $Ru_5(\mu_5\text{-}C{\equiv}C)(\mu\text{-}C_5H_4R)_2(dppm)(\mu_2\text{-}CO)_2(CO)_7$ (where R = H, Me), the new cluster $Ru_5(\mu_4\text{-}C{\equiv}C)Cp_2\text{-}(dppm)(\mu\text{-}CO)(CO)_9$ has also been isolated in the case of the Cp analogue. The X-ray structure of $Ru_5(\mu_4\text{-}C{\equiv}C)Cp_2(dppm)(\mu\text{-}CO)(CO)_9$ and the results of ^{13}CO labelling studies are presented [56]. A report describing the crystal and molecular structures of $Ru_3(CO)_9(\mu\text{-}dppm)[PPh_2(C_6H_4N{=}CHPh\text{-}2)]$ has appeared [57]. The migration of a phenyl group from a dppm ligand to an acetylide ligand has been observed in the thermolysis of $Ru_3(\mu\text{-}H)(\mu_3\text{-}C_2^tBu)(\mu\text{-}dppm)(CO)_7$. The major product isolated from this reaction is $Ru_3(\mu\text{-}H)(\mu_3\text{-}PPhCH_2PPh_2)(\mu_3\text{-}PhC_2^tBu)(CO)_6$, whose structure has been unequivocally established by X-ray analysis. Density functional and extended Hückel MO calculations reveal the presence of an unusual coordination of the alkyne ligand to the metallic frame, which is the result of the stereoelectronic asymmetry in the Ru_3 core [58]. Ph_2PH reacts with $Ru_3(CO)_{10}$(μ-dppm) at 98°C to afford $Ru_3(\mu\text{-}CO)(CO)_6(\mu\text{-}PPh_2)_2(\mu_3\text{-}CH_2PPh)$ in 20% yield. This cluster has been characterized in solution by ^1H- and ^{31}P-NMR spectroscopy, and in the solid state by X-ray crystallography. The Ru_3 product represents a rare example of a cluster containing a triply bridging CH_2PPh ligand and two doubly bridging PPh_2 moieties [59].

The phosphine-substituted cluster $[HRu_3(CO)_7(PCy_3)_2]^-$ has been synthesized from $[HRu_3(CO)_{11}]^-$ and excess PCy_3 in refluxing THF. The product represents a second example of a Ru_3 cluster possessing the rare electron count of 44 valence electrons. ^1H- and ^{31}P-NMR studies confirm the presence of two isomers in solution. The X-ray structure of one of the two solution isomers has been solved [60]. Thermolysis of $Ru_3(\mu_3\text{-}C{=}C{=}CPh_2)(\mu\text{-}dppm)(\mu\text{-}CO)(CO)_7$ initially produces $Ru_3(\mu_3\text{-}PPhCH_2PPh_2)(\mu_3\text{-}C_9H_5Ph_2)(CO)_6$, which on continued heating decarbonylates to the corresponding pentacarbonyl cluster. These products are the result of a phenyl group migration from the dppm ligand to the allenylidene ligand, which then undergoes a cyclization to furnish the 1,3-diarylindenyl moiety. The molecular structures of both clusters were crystallographically determined. Labelling studies using a di-4-tolylallenylidene ligand have provided valuable information concerning the course of these reactions [61]. The reaction of the (ferrocenylmethyl)phosphine ligand $CpFeCpCH_2PH_2$ with $Ru_3(CO)_{12}$ gives $Ru_3(CO)_9(\mu\text{-}H)_2(\mu_3\text{-}PCH_2CpFeCp)$ and $Ru_4(CO)_{11}(\mu_4\text{-}PCH_2CpFeCp)_2$, the former of which has been structurally characterized [62]. Thermolysis of $Ru_3(CO)_{12}$ with the bis(phosphine)hydrazine ligand $(MeO)_2PN(Me)N(Me)P(OMe)_2$ gives the simple substitution product $Ru_3(CO)_{10}[(MeO)_2PN(Me)N(Me)P(OMe)_2]$ as the initial product. This cluster then undergoes further reaction to give the known clusters $Ru_3(CO)_{11}[P(OMe)_3]$ and $Ru_4(CO)_{12}[\mu\text{-}N(Me)N(Me)]$, along with the phosphite-bridged cluster $Ru_3(CO)_9[\mu\text{-}P(OMe)_3]$. The X-ray structure of this latter cluster confirms the coordination of the

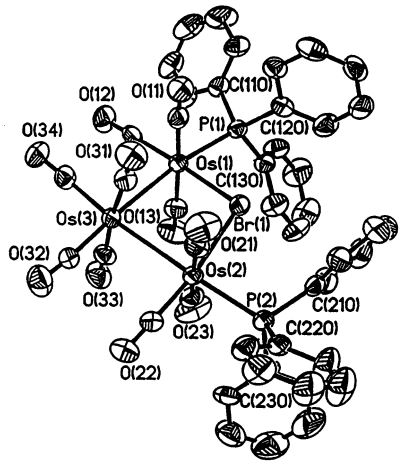

Fig. 4. X-Ray structure of $[Os_3(CO)_{10}(PPh_3)_2(\mu\text{-Br})]^+$. Reprinted with permission from Organometallics. Copyright 1999 American Chemical Society.

phosphorus center to one of the ruthenium atoms and the existence of an oxygen-bridged Ru–Ru vector by one of the methoxy groups [63]. The homogeneous hydrogenation of diphenylacetylene by $Ru_3(CO)_9P_3$ (where $P = PPh_3$, PEt_3) has been investigated, with $Ru_3(CO)_{10}(PEt_3)_2$ being observed in the catalytic reactions using PEt_3 as a ligand. This particular cluster was independently prepared and examined for its catalytic activity, where it exhibited superior hydrogenation activity relative to $Ru_3(CO)_9(PEt_3)_3$. The effect of H_2 pressure and substrate/cluster ratios on these reactions are discussed. The X-ray structure of $Ru_3(CO)_{10}(PEt_3)_2$ reveals that the two phosphines occupy equatorial positions on adjacent metal atoms so that they are *trans* to each other [64]. The X-ray diffraction structure of the elusive isomer of $Os_3(CO)_{10}(PPh_3)_2$ has been solved. Here the PPh_3 ligands are *cis* and *trans* with respect to the phosphine-substituted Os–Os edge. Comparisons of this isomer to that of the known *trans*, *trans* species are presented [65]. The reaction between the phosphine ligand 4′-diphenylphosphino-2,2′:6′,2″-terpyridine and $Os_3(CO)_{11}(MeCN)$ has been explored, and the product fully characterized in solution [66]. A study on the controlled photochemistry of $Ru_3(CO)_{12}$ and $Os_3(CO)_{12}$ has appeared. The nature of the final products is shown to be influenced by different solvents [67]. The results from a UV laser desorption/ionization mass spectrometry study of $Ru_3(CO)_{12-n}(PPh_3)_n$ (where $n = 1–3$) have been published [68]. Bromination of $Os_3(CO)_{10}(EPh_3)_2$ (where $E = P$, As) furnishes the cationic clusters $[Os_3(CO)_{10}(EPh_3)_2(\mu\text{-Br})]^+$, which may be crystallized as the $[Os(CO)_3Br_3]^-$ salts. The isolation of $[Os_3(CO)_{10}(EPh_3)_2(\mu\text{-Br})]^+$ provides the first direct evidence for the bromonium mechanism in the bromination of cluster complexes. VT ^{31}P-NMR data are discussed, and the X-ray structure of $[Os_3(CO)_{10}(PPh_3)_2(\mu\text{-Br})]^+$ (shown above in Fig. 4) has verified the cleavage of the Os–Os bond that is spanned by the bromine atom [69].

The build-up of a Ru_3 cluster in aqueous solution has been reported. Treatment of $[(\eta^6\text{-}C_6H_6)Ru(H_2O)_3]^{2+}$ with $[(\eta^6\text{-}C_6Me_6)_2Ru_2(\mu_2\text{-}H)_3]^+$ furnishes the oxo-capped cluster $[(\eta^6\text{-}C_6Me_6)_2(\eta^6\text{-}C_6H_6)Ru_3(\mu_2\text{-}H)_3(\mu_3\text{-}O)]^+$, whose molecular structure has been solved and confirmed the presence of the μ_3-oxo moiety. This Ru_3 cluster catalyzes the hydrogenation of aromatic compounds in aqueous solution under biphasic conditions [70]. The preparation and characterization of the trimetallic cyclopropenium cations $[M_3(\mu_3\text{-}C_3)]^+$ [where M=$CpFe(CO)_2$, $CpRu(CO)_2$, $CpMo(CO)_3$, $CpW(CO)_3$, $Re(CO)_5$] are described, and the X-ray structure of the iron derivative is presented. The X-ray data confirm the presence of a nearly equilateral C_3 ring with an iron atom bonded to each vertex. This same iron complex reacts with Super-Hydride and MeLi to give complex reaction mixtures [71]. The synthesis and X-ray structures of trimetallic boryloxycarbene complexes are reported. Treatment of the chloroboranes Cl_2BNR_2 [where R = $N'Bu(SiMe_3)$, $N(SiMe_3)_2$] with $[CpNi(CO)]^-$ or $[Fe_3(CO)_9(\mu_3\text{-}CO)_2]$ [2] affords the products $[Fe(CO)_3]_3(\mu_3\text{-}COBClNR_2)$ and $(CpNi)_3(\mu_3\text{-}COBClNR_2)$ [72]. The X-ray structure of $Os_3(\mu\text{-}H)(\mu\text{-}OCH_2CH_2OH)(CO)_{10}$ has been solved, and the triosmium core shows little structural effect on the glycol moiety [73]. $Fe_3(CO)_{12}$ reacts with tetraphenylhexapentaene to give $Fe_3(C_{15}H_{10})_2(CO)_8$, whose X-ray structure reveals the coordination of the bis(μ_3,η^2,η^2-diphenylallenylidene) moiety to an $Fe_3(CO)_8$ central core [74]. $Fe_3(CO)_{12}$ has been allowed to react with 1,4,7,10-tetraphenyl-cyclodecahexa-1,2,3,7,8,9-ene to give hexacarbonyl-η^2-(1η^2-1,2-ene-2η^2-3,4,5-allyl-1σ^1-5)diiron as the major product. The identity of the coordinated polyene was determined by X-ray crystallography [75]. The reaction of $Ru_3(CO)_{12}$ with ethyne in refluxing THF furnishes four complexes having the composition $Ru_2(CO)_m(C_2H_2)_n$ in low yield. Included in this report is the X-ray structure of $Ru_2(\mu,\eta^1,\eta^4\text{:}\eta^1,\eta^4\text{-}C_8H_8)(CO)_4$. The structures of the remaining products were assigned by spectroscopic methods [76].

Complex kinetics have been observed in the substitution reactions of $Os_3(CO)_9(\mu\text{-}C_4Ph_4)$ with small P-donor ligands. The osmacyclopentadiene ring in $Os_3(CO)_9(\mu\text{-}C_4Ph_4)$ activates the cluster towards associative ligand attack at the non-polyene bridged osmium atom by a factor of ca. 10^9 compared with reactions of the parent cluster $Os_3(CO)_{12}$. Three kinetically observable regimes that are dependent on the Tolman cone angle of the ligand have been found. Kinetic data, activation parameters, and reaction mechanisms are discussed [77]. $Ru_3(CO)_{12}$ reacts with $[nido\text{-}7\text{-}CB_{10}H_{13}]^-$ in refluxing THF to produce the anionic cluster $[Ru_3(CO)_8(\eta^5\text{-}7\text{-}CB_{10}H_{11})]^-$, which may be protonated with HBF_4 to furnish the corresponding neutral hydride cluster. The X-ray structure of $HRu_3(CO)_8(\eta^5\text{-}7\text{-}CB_{10}H_{11})$ consists of a triangle of ruthenium atoms, with the ancillary carborane moiety ligating a single ruthenium atom in an η^5 fashion. The anionic cluster may be functionalized with $CuCl(PPh_3)$ in the presence of $TlPF_6$ or $AgBF_4$ and PPh_3 to give $HRu_3(CO)_7(PPh_3)[\eta^5\text{-}10\text{-}M(PPh_3)\text{-}7\text{-}CB_{10}H_{10})]$ (where M = Cu, Ag). The X-ray structure of the Cu derivative is included in this report [78].

The ruthenium clusters $Ru_3(CO)_{10}[\mu_3\text{-}\eta^2\text{-}C_2(C{\equiv}CSiMe_3)_2]$ and $Ru_4(CO)_{12}[\mu_4\text{-}\eta^2\text{-}C_2(C{\equiv}CSiMe_3)_2]$ were obtained from the reaction between $Ru(CO)_5$ and 1,6-bis(trimethylsilyl)-1,3,5-hexatriyne. The molecular structures of both clusters were

determined. The same Ru_3 cluster may be isolated from $Ru_3(CO)_{11}(MeCN)$ and the triyne ligand. Treatment of $Ru_3(CO)_{10}[\mu_3\text{-}\eta^2\text{-}C_2(C{\equiv}CSiMe_3)_2]$ with $Ru(CO)_5$ is shown to afford the Ru_4 product, indicating that the Ru_3 cluster is a precursor to the final Ru_4 product [79]. A review on the synthesis, structures, and isolobal relationships of the *closo* clusters $M_3(CO)_8(RC_2R')_2$ has been published [80]. The reaction of $Ru_3(CO)_{10}(MeCN)_2$ and ethyne affords the known clusters $Ru_3(\mu_3\text{-}C_2H_2)(\mu\text{-}CO)(CO)_9$ and $Ru_3(\mu\text{-}H)(\mu_3\text{-}CCH)(CO)_9$, in addition to $Ru_4(\mu_4\text{-}C_2H_2)(CO)_{12}$, $Ru_5(\mu_5\text{-}CCH_2)(CO)_{15}$, and $Ru_6(\mu\text{-}H)(\mu_4\text{-}C)(\mu\text{-}CCMe)(\mu\text{-}CO)(CO)_{16}$. Five X-ray structures are presented, and schemes showing the possible course of reaction in the formation these clusters are discussed [81]. The five new fluorene-containing clusters $Ru_3(CO)_9(\mu\text{-}H)[\mu_3\text{-}\eta^1{:}\eta^2{:}\eta^2\text{-}CC(C_{13}H_9)]$, $Ru_3(CO)_7(\mu\text{-}CO)[\mu_3\text{-}\eta^1{:}\eta^2{:}\eta^4\text{-}(HOC_{13}H_8)CCHC(C_{13}H_8OH)CH]$, $Ru_4(CO)_{10}(\mu\text{-}CO)(\mu_3\text{-}OH)(\mu_3\text{-}\eta^1{:}\eta^2{:}\eta^2\text{-}C_{13}H_9CCH)$, $Ru_5(CO)_{11}(\mu\text{-}H)(\mu\text{-}CO)(\mu_3\text{-}OH)(\mu_5\text{-}\eta^1{:}\eta^1{:}\eta^2{:}\eta^2{:}\eta^6\text{-}C_{13}H_7CHC)$, and $Ru_6(CO)_{15}(\mu_5\text{-}\eta^1{:}\eta^1{:}\eta^2{:}\eta^3{:}\eta^6\text{-}C_{13}H_7CHC)$ have been isolated from the reaction between 9-ethynylfluoren-9-ol and $Ru_3(CO)_{12}$ in refluxing THF. The X-ray structures of all five cluster products have been solved and are discussed relative to the nature of the coordination mode adopted by the ancillary fluorene ligand [82]. Six new hexaruthenium clusters have been isolated from the reaction between $Ru_3(CO)_{12}$ and the ligands 1-ethynylcyclopentanol, 1-ethynylcycloheptanol, and 1-ethynylcyclooctanol. The molecular structures of the new clusters were established by solution methods and X-ray crystallography [83]. The diyne ligand 1,4-bis(1-hydroxycyclopentyl-1,3-butadiyne) reacts with $Ru_3(CO)_{12}$ in refluxing $CHCl_3$ to give the new clusters $Ru_3(CO)_7(\mu\text{-}CO)(\mu_3\text{-}\eta^2{:}\eta^3{:}\eta^3\text{-}C_{28}H_{34}O_3)$ (two separate isomers) and $Ru_3(CO)_8(\mu_3\text{-}\eta^2{:}\eta^2{:}\eta^4\text{-}C_{28}H_{32}O_2)$. These three products have been fully characterized in solution and by X-ray crystallography. The isomeric clusters $Ru_3(CO)_7(\mu\text{-}CO)(\mu_3\text{-}\eta^2{:}\eta^3{:}\eta^3\text{-}C_{28}H_{34}O_3)$ differ only in the spatial positioning of the pendant alkyne moiety in the C_8 hydrocarbyl fragment. The same butadiyne ligand reacts with $Ru_3(CO)_{10}(MeCN)_2$ to furnish $Ru_3(CO)_9(\mu\text{-}CO)(\mu_3\text{-}\eta^1{:}\eta^1{:}\eta^2\text{-}C_{14}H_{18}O_2)$, whose molecular structure was ascertained by X-ray methods [84]. The alkyne clusters $Os_3(CO)_{10}(\mu_3\text{-}\eta^2\text{-}C_{14}H_{20})$ and $[Os_3(CO)_{10}]_2(\mu_3,\mu_3\text{-}\eta^2,\eta^2\text{-}C_{14}H_{20})$ have been obtained from $Os_3(CO)_{10}(MeCN)_2$ and cyclotetradeca-1,8-diyne. Thermolysis of the former product cluster gives $(\mu\text{-}H)Os_3(CO)_9(\mu_3\text{-}\eta^3\text{-}C_{14}H_{19})$ via C–H bond activation, while photolysis of the same cluster in the presence of added diyne yields $Os_3(CO)_9[\mu\text{-}\eta^4\text{-}C_4(C_{12}H_{20})_2]$. The osmacyclopentadienyl fragment in this latter cluster was confirmed by X-ray diffraction analysis. When $Fe_3(CO)_{12}$ is allowed to react with the diyne ligand, $Fe_3(CO)_9(\mu_3\text{-}\eta^2\text{-}C_{14}H_{20})$ was observed as the major product, which upon heating undergoes cluster fragmentation. The X-ray structure of $(\mu\text{-}H)Os_3(CO)_9(\mu_3\text{-}\eta^3\text{-}C_{14}H_{19})$ (Fig. 5) shows the presence of an osmium triangle and a coordinated allene moiety to two of the three osmium atoms [85].

A detailed study of electron transfer on the infrared vibrational time scale in mixed-valence ruthenium clusters has been published. Intramolecular electron transfers within the mixed-valence states of $Ru_3(\mu_3\text{-}O)(\mu\text{-}OAc)_6(CO)(L)(\mu\text{-}L')Ru_3(\mu_3\text{-}O)(\mu\text{-}OAc)_6(CO)(L)$ (where L = pyridine ligand; L′ = bpy, 1,4-pyrazine) have been measured. The electronic coupling (H_{AB}) between the two Ru_3 clusters

varies from 80 to 440 mV, and the magnitude of H_{AB} has been shown to strongly influence the IR spectra of the singly reduced (-1) mixed-valence state. The electron-transfer dynamics have been evaluated via Bloch equation simulation of the IR band shape of the CO ligands [86]. Seven new oxo-capped Ru_3 clusters have been prepared and their electrochemistry investigated. These clusters have the general form $Ru_3(O)(AcO)_6(CNC_6H_3Me_2\text{-}2,6)(L)_{3-n}$ (where L = CO, various nitrogen ligands) [87]. Charge separation in an Os_3 cluster zwitterion has been revealed by time-resolved microwave conductivity (TRMC) studies. Photolysis of $Os_3(CO)_{10}$(μ-diimine) clusters in the presence of an added P- or N-ligand affords an intermediate zwitterion as a result of metal–metal bond cleavage, followed by ligand capture. The dipole moment of the intermediate zwitterion has been measured by TRMC experiments [88]. Stable radical anions derived from clusters containing an ancillary *ortho*-metallated μ-diimine ligand have been observed. The spectroelectrochemical data and theoretical calculations at the extended Hückel level are discussed [89]. Photolysis of $Os_3(CO)_{10}$(pyridine-2-carbaldehyde-*N′*-*R* imine) clusters with visible light ultimately affords zwitterionic intermediates upon coordination of the pendant Lewis base. The photochemistry and photophysics for zwitterion formation are discussed [90]. (*S*)-Nicotine and (*R*)-1-(4-pyridyl)ethanol react with $Os_3(CO)_{10}(MeCN)_2$ to give diastereomeric *ortho*-metallated products. X-ray diffraction structures and circular dichroism data are presented and discussed [91]. The cluster-mediated conversion of diphenylacetylene to μ-phenylcinnamaldehyde has been studied by using a Ru_3 cluster containing a hemilabile ancillary ligand. Treatment of Ru_3(μ-H)(μ-MeNpy)$(CO)_9$ with diphenylacetylene leads to the alkenyl cluster Ru_3(μ-MeNpy)(μ-PhC=CHPh)$(CO)_8$, whose molecular structure has

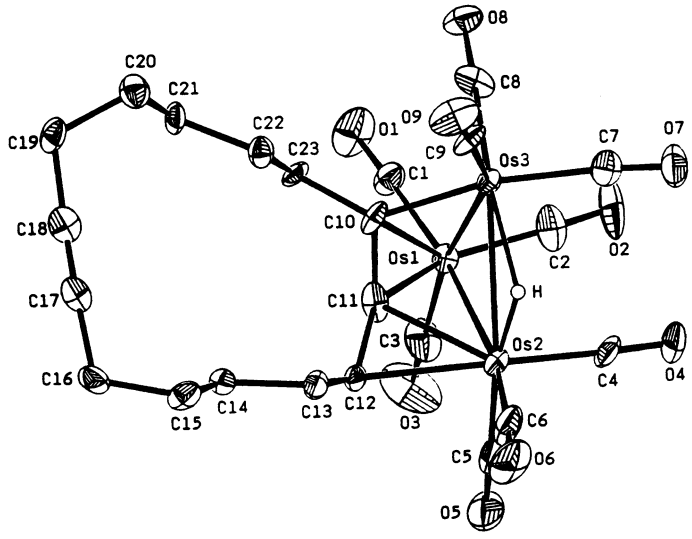

Fig. 5. X-Ray structure of (μ-H)$Os_3(CO)_9(\mu_3\text{-}\eta^3\text{-}C_{14}H_{19})$. Reprinted with permission from Organometallics. Copyright 1999 American Chemical Society.

been confirmed by X-ray analysis. The alkenyl-substituted cluster reacts with added PPh_3 via CO insertion into the Ru-alkenyl bond to afford the propenoyl clusters $Ru_3(\mu\text{-MeNpy})(\mu\text{-O=C–PhC=CHPh})(PPh_3)(CO)_7$ and $Ru_3(\mu\text{-MeNpy})(\mu\text{-O=C–PhC=CHPh})(PPh_3)_2(CO)_6$. Use of CO in place of PPh_3 gives $Ru_3(\mu\text{-MeNpy})(\mu\text{-O=C–PhC=CHPh})(CO)_9$, which is shown to release μ-phenylcinnamaldehyde upon treatment with syn gas. Mechanistic sequences accounting for cluster catalysis are presented [92]. MeCHO is shown to react with $H(\mu\text{-H})Os_3(CO)_{10}(NH_3)$ to give the imine cluster $H(\mu\text{-H})Os_3(CO)_{10}(HN{=}CHMe)$. Spectroscopic data indicate that the imine ligand occupies a terminal position on the cluster. The stereochemistry of the product is determined by an unconventional hydrogen-bond interaction between the N–H moiety and the terminal Os–H group. Such an intramolecular Os–H···H–N hydrogen bond is supported by ^{1}H-NMR spin lattice relaxation (T_1) studies [93]. Excess imidazo(1,2-a)pyridine reacts with $Os_3(CO)_{10}(MeCN)_2$ to give $(\mu\text{-H})Os_3(CO)_{10}(\mu\text{-1,2-}\eta^2\text{-}C_7H_5N_2)$ and $(\mu\text{-H})Os_3(CO)_{10}(\mu\text{-1,7-}\eta^2\text{-}C_7H_5N_2)$. Solution spectroscopic data and X-ray crystallography have ascertained the coordination mode adopted by the heterocyclic ligand. The reactivity of the same heterocycle with $Os_3(CO)_{11}(MeCN)$ is also presented [94]. The clusters $(\mu\text{-H})Os_3(CO)_{10}[NC_3HS\text{–}N{=}N\text{–}C_{10}H_6(OH)]$ and $(\mu\text{-H})Os_3(CO)_9[\mu\text{-}\eta^3\text{-}NC_3H_2S(N{=}N)C_{10}H_4(O)]$ have been synthesized from $Os_3(CO)_{10}(MeCN)_2$ and 1-(2-thiazolylazo)-2-naphthol [95].

The cluster $HRu_3(CO)_9[NS(O)MePh]$ reacts with two equivalents of 2-butyne to give the dienonyl species $Ru_3(CO)_7[NS(O)MePh](HCMeCMeCMeCMeCO)$ and the isomeric clusters $Ru_3(CO)_8[NS(O)MePh](HCMeCMe)$. When the same reaction was carried out at 100°C, only the diendiyl cluster $Ru_3(CO)_8(CMeCMeCMeCMe)$ was isolated. Two X-ray structures accompany this report [96]. The mononuclear compound Ru(CO)(AcO)(tpa) has been obtained from the reaction between $Ru_3(CO)_{12}$ and tpa in acetic acid [97]. The reductive coupling of alkynes has been observed in the reaction of $M_3(\mu\text{-H})_2(\mu_3\text{-X})(CO)_9$ (where M = Ru, Os; X = $NSO_2C_6H_4Me$-4, S) with terminal alkynes to furnish the diene products $M_3(C_4H_4R_2)(\mu_3\text{-X})(CO)_8$. The ancillary diene ligand is bound to the ruthenium cluster in a $\mu\text{-}\eta^2,\eta^2$ fashion and by an η^4 mode in the case of the osmium cluster [98]. A report describing an electrospray mass spectrometry study of polynuclear clusters in the presence of azide ions has been published. Most of the complexes give appropriate isocyanate-containing anions by the conversion of a CO ligand to a NCO group with elimination of N_2. For hydride clusters, the azide ion may function as a base, abstracting H^+ and generating $[\text{cluster-H}]^-$ ions [99]. The reactivity of $Os_3(CO)_9(\mu_3\text{-}\eta^2\text{-}C_{13}H_8N)(\mu\text{-H})$ in ligand substitutions and the functionalization of the heterocyclic ligand in this same cluster are reported. PPh_3 reacts with this Os_3 cluster to produce $Os_3(CO)_9(\mu\text{-}\eta^2\text{-}C_{13}H_8N)(\mu\text{-H})(PPh_3)$, which undergoes thermal and photochemical decarbonylation to give $Os_3(CO)_8(\mu_3\text{-}\eta^3\text{-}C_{13}H_8N)(\mu\text{-H})(PPh_3)$. This octacarbonyl cluster exhibits a σ-π-vinyl bonding mode for the C(9)=C(10) double bond and not the expected $\mu_3\text{-}\mu^2$ electron-deficient bonding mode, as confirmed by X-ray analysis (Fig. 6). The selectivity for hydride addition to C(9) of the heterocyclic ligand and lithium isobutyrile nitrile addition to the 3,4 double bond is reported [100].

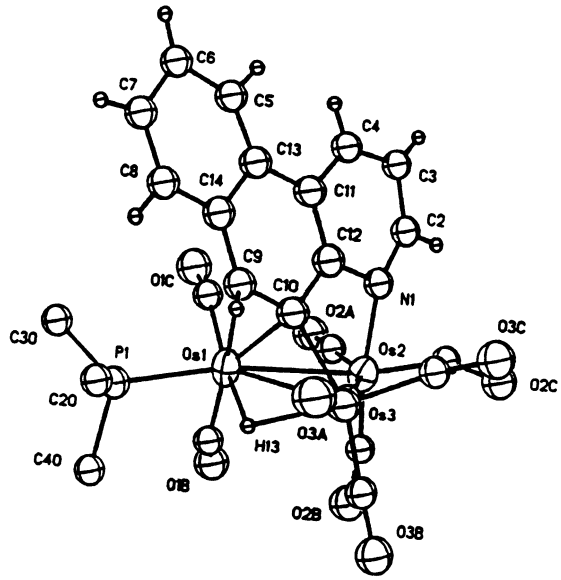

Fig. 6. X-Ray structure of $Os_3(CO)_8(\mu_3\text{-}\eta^3\text{-}C_{13}H_8N)(\mu\text{-}H)(PPh_3)$. Reprinted with permission from Organometallics. Copyright 1999 American Chemical Society.

A review discussing the recent developments of tellurium- and selenium-containing iron clusters has appeared [101]. The synthesis and X-ray structure of $Fe_3(CO)_6(\mu_3\text{-}Se)[\mu\text{-}AsMe\{CpFe(CO)_2\}]_2(\mu\text{-}CO)$ have been published. The title cluster has been prepared from $Fe_3(CO)_9(\mu_3\text{-}Se)(\mu_3\text{-}AsMe)$ and $CpCo(CO)_2$ [102]. Refluxing $CpRu(PPh_3)_2(SCH_2CH{=}CH_2)$ in toluene leads to C–S bond cleavage and formation of $(CpRu)_3(\mu_3\text{-}S)_2(\mu\text{-}SCH_2CH{=}CH_2)$ in moderate yield. This Ru_3 cluster was fully characterized in solution and its molecular structure was established by X-ray methods [103]. The ring opening of 1,3-dithietane-1,1-dioxide by an Os_3 cluster is discussed. Use of $Os_3(CO)_{10}(MeCN)_2$ at r.t. leads to the cluster $Os_3(CO)_{10}(\mu\text{-}CH_2SCH_2SO_2)$, which when refluxed in heptane undergoes fragmentation to $Os_2(CO)_6(\mu\text{-}CH_2SCH_2SO_2)$. The molecular structure of each product was determined by X-ray crystallography [104]. 3,6-Dihydro-1,2-dithiin reacts with $Os_3(CO)_{10}(MeCN)_2$ at 0°C to give the isomeric clusters $Os_3(CO)_{10}(\mu_3\text{-}SCH_2CH{=}CHCH_2S)$ and $Os_3(CO)_{10}(\mu\text{-}SCH_2CH{=}CHCH_2S)$. Thermolysis of the former product cluster furnishes the latter $\mu\text{-}SCH_2CH{=}CHCH_2S$ isomer and $Os_6(CO)_6(\mu\text{-}SCH_2CH{=}CHCH_2S)$; however, thermolysis of $Os_3(CO)_{10}(\mu\text{-}SCH_2CH{=}CHCH_2S)$ does not afford any of the $\mu_3\text{-}SCH_2CH{=}CHCH_2S$ species. All complexes were characterized by IR and ^{1}H-NMR spectroscopy, and by X-ray crystallography in the case of two Os_3 clusters [105]. Treatment of $Os_3(CO)_{10}(MeCN)_2$ with 2-vinyltetrahydrothiophene at r.t. produces $Os_3(CO)_{10}(\mu SCH_2CH_2CH{=}CHCH{=}CH_2)(\mu\text{-}H)$ and $Os_2(CO)_6[\mu\text{-}\mu^4\text{-}S(CH_2)_3CH{=}CHCH_2](\mu\text{-}H)$. X-ray analysis of the Os_3 product verifies the coordination of the hexadienethiolate ligand to a triangular triosmium frame. Ring opening

of the 2-vinyltetrahydrothiophene substrate by the Os_3 cluster occurs exclusively at the vinyl-substituted carbon atom [106]. C–H bond cleavage is observed in the reaction between $Os_3(CO)_{10}(MeCN)_2$ and benzo[b]thiophene, giving $Os_3(\mu\text{-}H)(CO)_{10}(\mu\text{-}C_8H_5S)$ and $Os_3(\mu\text{-}H)_2(CO)_9(\mu_3\text{-}C_8H_4S)$. The cluster complex $Os_3(CO)_{10}(\mu\text{-}C_8H_6S)$ was also observed as a result of C–S bond cleavage. Thermolysis of the monohydride product is shown to furnish the latter two Os_3 clusters. Similar reactivity is observed in the reaction between dibenzothiophene and $Os_3(CO)_{10}(MeCN)_2$. Mechanistic schemes, spectroscopic data, and the X-ray structure of $Os_3(\mu\text{-}H)_2(CO)_9(\mu_3\text{-}C_{12}H_6S)$ are presented [107]. $Ru_3(CO)_{12}$ reacts with benzothiazole in refluxing THF to give $Ru_3(\mu\text{-}H)(CO)_{10}(\mu\text{-}2,3\text{-}\eta^2\text{-}NSC_7H_4)$ and $Ru_3(\mu\text{-}H)(CO)_9(\mu_3\text{-}1,2,3\text{-}\eta^3\text{-}NSC_7H_4)$. The molecular structure of the former cluster shows that the benzothiazolide moiety is coordinated to the Ru_3 frame via the imine nitrogen and the C-2 carbon atoms. Spectroscopic data on $Ru_3(\mu\text{-}H)(CO)_9(\mu_3\text{-}1,2,3\text{-}\eta^3\text{-}NSC_7H_4)$ support benzothiazolide ligand coordination through the sulfur, imino nitrogen, and the C-2 carbon atoms. The latter product cluster is obtained when the former product cluster is heated in cyclohexane solution. Use of pyrimidine-2-thione and benzimidazole-2-thione as ligands in the reaction with $Ru_3(CO)_{12}$ is also described [108]. Ring-opening reactions of thiomorpholine and thiazolidine with $Ru_3(CO)_{12}$ are reported. Details concerning the X-ray structures of $Ru_3(\mu\text{-}H)(CO)_9(\mu\text{-}\eta^2\text{-}SCH_2CH_2NH_2)$ and $Ru_2(CO)_6(\mu\text{-}\eta^3\text{-}SCH_2CH_2NHCH_2)$ have been published [109]. The interaction of triosmium clusters with pyridinethiols has been explored. Treatment of pyrimidine-2,4-dithiol and pyridine-2-thiol with $Os_3(CO)_{11}(MeCN)$ yields $[Os_3(\mu\text{-}H)(CO)_{10}]_2(\mu\text{-}S_2C_4H_2N_2)$ and $Os_3(\mu\text{-}H)(CO)_{10}(\mu\text{-}SC_5H_4N)$, respectively. Each product contains a chelating μ,η^1 thiolate ligand and a μ-hydride group across a common edge of the osmium triangle, as confirmed by X-ray crystallography [110]. The clusters $[Fe_3(CO)_9(\mu_3,\eta^2\text{-}SO_2)]^{2-}$ (Fig. 7) and $[Fe_3(CO)_8(\mu\text{-}SO_2)(\mu_3\text{-}S)]^{2-}$ have been isolated from the reaction of SO_2 with $[MFe_3(CO)_9]^{2-}$ (where M = Cr, Mo, W). X-ray diffraction analyses confirm the identity and coordination mode exhibited by the ancillary sulfur ligand(s). A reaction scheme illustrating the course of the reactivity in these clusters is discussed [111].

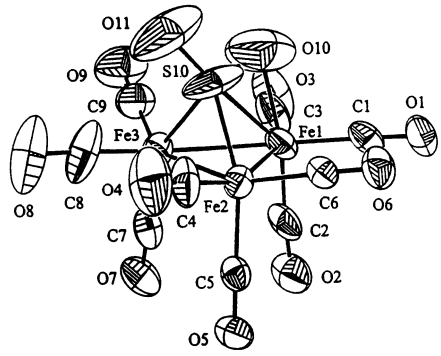

Fig. 7. X-Ray structure of $[Fe_3(CO)_9(\mu_3,\eta^2\text{-}SO_2)]^{2-}$. Reprinted with permission from Inorganic Chemistry. Copyright 1999 American Chemical Society.

The reaction of $[Cp^*RuCl]_4$ with several nucleophilic carbene ligands has been investigated, and the resulting products have been analyzed by structural and thermochemical methods [112]. Ruthenium methylene/silyl complexes exhibiting the stoichiometry $Cp^*_2Ru_2(\mu\text{-}CH_2)(SiR_3)(\mu\text{-}Cl)$ have been synthesized from $[Cp^*RuCl]_4$ and the appropriate $Mg(CH_2SiR_3)_2$ reagent [113]. The synthesis, X-ray structure, and redox behavior of the sulfido-bridged cluster $[Fe_3(CO)_9\{\mu_3\text{-}SFeCp(CO)_2\}]^-$ have been published. The product cluster was isolated from the reaction between $[CpFe(CO)_2(THF)]^+$ and $[Fe_3(CO)_9(\mu_3\text{-}S)]$.[2] Thermolysis of this Fe_4 cluster yields $[CpFe(CO)_2]_2$, $[Fe_3(CO)_9(\mu_3\text{-}S)]^{2-}$, and $[Fe_5(CO)_{14}(\mu_3\text{-}S)_2]^{2-}$ [114]. A Ru_4 cluster possessing a facial-bound indenyl-type ligand has been synthesized and structurally characterized. The X-ray structure of $(\mu_3\text{-}\eta^1\text{:}\eta^3\text{:}\eta^5\text{-}3,4,5\text{-trihydroacenaphthylenyl})Ru_4H(CO)_9$ shows the presence of a nine-electron donor ligand, where one ruthenium atom is bound by a μ-Cp ligand and two other ruthenium atoms are substituted by the remaining arene carbon atoms in an $\eta^1\text{:}\eta^3$-bonding mode [115]. The catalytic activity of polynuclear ruthenium complexes in benzo[b]thiophene hydrodesulfurization reactions has been explored at elevated temperatures under 100 bar of H_2 gas. The observed reduction products were 2,3-dihydrobenzo[b]thiophene and 2-ethylthiophenol, with $H_4Ru_4(CO)_8(PPh_3)_4$ exhibiting the greatest activity [116].

The ferrocenyl-substituted ruthenium clusters $Ru_4(CO)_{12}[\mu_4\text{-}\eta^1,\eta^1,\eta^2,\eta^2\text{-}CpFe(C_5H_4CCCHO)]$ and $Ru_3(CO)_8[\mu_3\text{-}\eta^1,\eta^2,\eta^4\text{-}\{CpFe(C_5H_4CCCHO)\}_2]$ have been synthesized from $CpFe(C_5H_4CCCHO)$ and $Ru_3(CO)_{12}$ in refluxing cyclohexane. X-ray analysis of the Ru_4 cluster shows a ferrocenyl carboxaldehyde bound to a Ru_4 butterfly skeleton via a $\mu_4\text{-}\eta^1,\eta^1,\eta^2,\eta^2$ coordination mode. Thermolysis of this cluster in toluene gives the rare pentaruthenium cluster $Ru_5(CO)_{13}(\mu\text{-}H)(\mu_5\text{-}C)[\eta^2\text{-}\eta^1,\eta^1\text{-}CpFe(C_5H_4C)]$, whose X-ray structure contains a carboferrocenyl moiety tethered to the ruthenium frame in a $\eta^2\text{-}\eta^1,\eta^1$ fashion. The fluxional behavior and electrochemical properties of the Ru_5 cluster are presented [117]. The reaction of $Os_4(\mu\text{-}H)_4(CO)_{10}(MeCN)_2$ with 4-phenylazopyridine yields the new clusters $Os_4(\mu\text{-}H)_4(CO)_{11}(NC_5H_4N{=}NPh)$ and $Os_4(\mu\text{-}H)_4(CO)_{10}(MeCN)(NC_5H_4N{=}NPh)$. The former product exists as a pair of isomers in solution, which differ in the location of the bridging hydride ligands about the cluster core. The X-ray structures of both clusters have been solved [118]. $Cp_4Fe_4(CO)_4$ reacts sequentially with RLi and HBF_4 to give $Cp_3Fe_4(CpR)(CO)_4$ (where R = Me, Bu, Ph) in moderate yields. Use of LDA and bromoferrocene allows for the synthesis of the ferrocenylated cluster $Cp_3Fe_4(CO)_4(C_5H_4)(C_5H_4)FeCp$ and the double cluster $[Cp_3Fe_4(CO)_4(C_5H_4)]_2$. Related reactions are discussed, and all new compounds have been fully characterized in solution by IR and-NMR spectroscopy [119]. The activated cluster $Os_4(\mu\text{-}H)_4(CO)_{11}(MeCN)$ reacts with monopyridyl ligands to afford the monosubstituted clusters $Os_4(\mu\text{-}H)_4(CO)_{11}(N)$ (where N = various pyridine ligands). Use of $Os_4(\mu\text{-}H)_4(CO)_{10}(MeCN)_2$ with bidentate nitrogen ligands leads to $Os_4(\mu\text{-}H)_4(CO)_{10}(N\text{–}N)$ (where N–N=bpy, 1,10-phen, dmdpp, dpbpy, dppz) [120]. Thermolysis of $Ru_4(\mu_4\text{-}C_2H_2)(CO)_{12}$ in toluene furnishes the cluster $Ru_4(\mu_4\text{-}C_2H_2)(CO)_9(\mu^6\text{-}PhMe)$. The crystal and molecular structure have been determined at r.t. and at 153 K. At low temperature, the Ru_4 structure is nicely ordered with

the acetylene ligand sitting between the wing-tip ruthenium atoms and an η^6-PhMe ligand attached to one of the wing-tip ruthenium atoms. The disorder observed in the structure determined at r.t. is discussed [121]. Acetylene incorporation into the spiked framework of phosphinidene and arsinidene clusters is reported. The reaction of $Ru_4(CO)_{13}(\mu\text{-}H)_2(\mu_4\text{-}ECF_3)$ (where E = P, As) with RC≡CR (where R = Ph, H) takes place under mild conditions to afford the square-planar clusters $Ru_4(CO)_9(\mu\text{-}CO)_2(\mu_4\text{-}ECF_3)(RC_2R)$, where the alkyne ligands are attached to the metal square by $2\sigma + 4\pi$ bonds, as verified by X-ray analysis. Use of 2-butyne results in metal skeletal rearrangement and P–C bond formation to yield $Ru_4(CO)_{10}(\mu\text{-}CO)_2[CF_3PC(Me)C(Me)]$ and alkyne dimerization at the spiked ruthenium atom to give $Ru_4(CO)_9(\mu\text{-}CO)_2(\mu_4\text{-}ECF_3)(C_4Me_4)$. The X-ray structure of the phosphinidene cluster shows the presence of a metallocyclic RuC_4Me_4 ring [122]. The reaction of the pyridyl-containing ligands dpp, bpm, and dpq with $Os_4(\mu\text{-}H)_4(CO)_{10}(MeCN)_2$ produces the expected disubstituted clusters $Os_4(\mu\text{-}H)_4(CO)_{10}(N\text{–}N)$. All three products have been structurally characterized by X-ray crystallography. The protonation chemistry of the dpp derivative is also discussed [123].

The reaction between Fp*-$(C\equiv C)_n$-Fp* (where $n = 3$, 4) and $Fe_2(CO)_9$ leads to C≡C bond cleavage and formation of the bis(μ_3-alkylidyne) clusters Fp*–C≡C-μ_3-$CFe_3(CO)_9$-μ_3-$C(C\equiv C)_{n-2}$–Fp*. The molecular structure of one product cluster accompanies this report [124]. The open cluster $Ru_5(\mu_5\text{-}C_2PPh_2)(\mu\text{-}PPh_2)(CO)_{13}$ reacts with dppm to give the new cluster $Ru_5(\mu_5\text{-}C_2PPh_2)(\mu\text{-dppm})(\mu\text{-}PPh_2)(CO)_{11}$, whose X-ray structure reveals the presence of seven Ru–Ru bonds and a dppm ligand that bridges an outer Ru–Ru vector, adjacent to that bridged by the phosphido ligand [125]. Butadiene reacts with $Ru_5(\mu_5\text{-}C_2)(\mu\text{-}SMe)_2(\mu\text{-}PPh_2)_2(CO)_{11}$ to produce $Ru_5(\mu_3\text{-}C_6H_6)(\mu_3\text{-}SMe)_2(\mu\text{-}PPh_2)_2(CO)_{10}$. This 80-electron cluster contains a coordinated $\mu_3\text{-}\eta^1\text{:}\eta^1\text{:}\eta^2$-cyclohex-1-en-4-yne ligand, as confirmed by X-ray diffraction analysis. Structural comparisons of this product to other clusters having an 80-cluster valence count are presented and discussed [126]. The formation of butatrienylidene complexes have been observed from the reaction between $C_2(SiMe_3)_2$ and $Ru_5(\mu_5\text{-}C_2)(\mu\text{-}SMe)_2(\mu\text{-}PPh_2)_2(CO)_{11}$. Presented in this report are the X-ray structures of $Ru_5[\mu_5\text{-}CC\{C_2(SiMe_3)\}C(SiMe_3)C(SiMe_3)](\mu_3\text{-}SMe)(\mu\text{-}PPh_2)_2(CO)_{10}$, $Ru_5(\mu_5\text{-}CCCCH_2)(\mu\text{-}SMe)_2(\mu\text{-}PPh_2)_2(CO)_{11}$, and $Ru_5(\mu_5\text{-}CCCCH_2)(\mu_3\text{-}SMe)(\mu\text{-}SMe)(\mu\text{-}PPh_2)_2(CO)_{10}$ [127]. The dicarbide cluster $Ru_5(\mu_5\text{-}C_2)(\mu\text{-}SMe)_2(\mu\text{-}PPh_2)_2(CO)_{11}$ has been allowed to react with diphenylethyne and 2-butyne. In the case of PhC≡CPh, the major products isolated were $Ru_5(\mu_5\text{-}CCCPhCPh)(\mu\text{-}SMe)_2(\mu\text{-}PPh_2)_2(CO)_{10}$ and $Ru_5(\mu_5\text{-}CCCPhCPh)(\mu_3\text{-}SMe)(\mu\text{-}SMe)(\mu\text{-}PPh_2)_2(CO)_9$. The only product isolated from the reaction with 2-butyne was $Ru_5(\mu_5\text{-}CCCMeCMe)(\mu_3\text{-}SMe)(\mu\text{-}SMe)(\mu\text{-}PPh_2)_2(CO)_9$. The interconversion pathways of these clusters under pyrolysis conditions are discussed. The X-ray structures of the diphenylacetylene-derived clusters accompany this report [128]. $Ru_5(\mu_5\text{-}CCCHCR)(\mu\text{-}SMe)_2(\mu\text{-}PPh_2)_2(CO)_{10}$ (where R = Ph, ^{t}Bu, $SiMe_3$) have been obtained from the reaction between terminal alkynes and $Ru_5(\mu_5\text{-}C_2)(\mu\text{-}SMe)_2(\mu\text{-}PPh_2)_2(CO)_{11}$. The regiospecific coupling of the C_2 moiety and the alkyne ligand leads to a CCCHCR ligand that forms a metallocyclic ring with one of the

ruthenium atoms. Pyrolysis of these products gives $Ru_5(\mu_5\text{-CCCHCR})(\mu\text{-SMe})_2(\mu\text{-PPh}_2)_2(CO)_{10}$ and $Ru_5(\mu_5\text{-CCCHCR})(\mu_3\text{-SMe})(\mu\text{-SMe})(\mu\text{-PPh}_2)_2(CO)_9$. The structures of five clusters were established by X-ray crystallography [129]. The double addition of 1,4-diphenylbuta-1,3-diyne to $Ru_5(\mu_5\text{-C}_2)(\mu\text{-SMe})_2(\mu\text{-PPh}_2)_2(CO)_{11}$ has been found to give a cluster containing an unusual multi-branched C_{10} ligand [130].

The UV laser desorption/ionization time-of-flight mass spectra of $Os_6(CO)_{18}$ have been recorded in both the positive and negative mode. The major products of the laser desorption/ionization of $Os_3(CO)_{10}(MeCN)_2$ and $H_2Os_3(CO)_{10}$ were found to be $Os_6(CO)_{18}$ and related Os_6 clusters. The high-yield synthesis of $Os_6(CO)_{18}$ using this technique is discussed [131]. The kinetics for P-ligand substitution in the planar 'raft' cluster $Os_6(CO)_{20}(MeCN)$ have been studied. Replacement of MeCN by the P ligand proceeds by the adducts $Os_6(CO)_{20}(MeCN)(P)$, which release MeCN in a relatively slow step. The intermediate adduct clusters $Os_6(CO)_{20}(MeCN)(P)$ are formed reversibly, and it is shown that the equilibrium and rate constants vary systematically with the electronic and steric nature of the P ligand. The exceptional substitutional lability in $Os_6(CO)_{20}(MeCN)$ to P-ligand attack is shown to be 10^5 times greater than that of $Os_3(CO)_{11}(MeCN)$ [132]. The reduction of SO_2 to SO by either CO or H_2 on a Ru_6 cluster has been demonstrated. Treatment of $[Ru_6C(CO)_{15}(\mu\text{-SO}_2)]^{2-}$ with CO at elevated temperature gives $Ru_6C(CO)_{16}S$, while reaction with H_2 gives the known triruthenium cluster $Ru_3(CO)_9(\mu\text{-H})_2(\mu_3\text{-S})$ and the new clusters $Ru_6C(CO)_{16}(H)_2S$ and $Ru_6C(CO)_{16}(H)_4S$. The three Ru_6 clusters were characterized in solution and by X-ray crystallography [133]. The paracyclophane-substituted clusters $Ru_6C(CO)_{14}(C_{16}H_{15}NH_2)$ and $Ru_6C(CO)_{14}(C_{16}H_{15}Br)$ have been synthesized and fully characterized in solution by IR and NMR spectroscopy. The use of COSY spectroscopy in the characterization of the bromo analogue is discussed. The X-ray data from the amino derivative are presented, and structural comparisons to other suitable arene-substituted clusters are described [134]. New $Ru_6C(CO)_{14}$-[2.2]-cyclophane and $Ru_6C(CO)_{14}$-[2.2.2]-cyclophane clusters have been prepared and examined in redox coupling reactions. Two X-ray structures are included in this report [135]. The new raft clusters $Os_6(CO)_{16}(\mu_3\text{-}\eta^2\text{-}C_5H_4NS)_2$ and $Os_6(CO)_{17}(\mu\text{-H})(\mu_4\text{-}\eta^2\text{-}C_5H_4NS)$ have been obtained from the reaction between $Os_6(CO)_{16}(MeCN)_2$ and 2-Aldrithol. The CV behavior of the former cluster shows two metal-based, one-electron reduction couples and an irreversible ligand-based anodic redox wave. X-ray studies reveal that these raft clusters contain 'ladder'-type and edge-fused raft cluster cores. The utility of these clusters to serve as models for substrates adsorbed onto metal surfaces is discussed [136]. Cyclic thioethers have been allowed to react with $Os_6(CO)_{16}(MeCN)_2$ to afford a variety of Os_6 clusters. All products were fully characterized in solution, and the X-ray structures of nine compounds were determined [137].

The activated cluster $Os_7(CO)_{19}(MeCN)_2$ reacts with 1,4-thioxane in CH_2Cl_2 to give the air-stable clusters $Os_7(CO)_{16}[\mu\text{-S}(CH_2)_2OCH_2C^aH_2(S\text{-}C^a)]_2$, $Os_7(CO)_{17}[\mu\text{-S}(CH_2)_2OCH_2C^aH_2(S\text{-}C^a)][S(CH_2)_2OCH_2C^aH_2(S\text{-}C^a)]$, and $Os_7(CO)_{19}[\mu\text{-S}(CH_2)_2OCH_2C^aH_2(S\text{-}C^a)]$. The metal skeletons of these clusters exhibit a winding helix made up of four tetrahedral sharing three common faces. The redox properties of these clusters are contrasted with that of the parent cluster $Os_7(CO)_{21}$ [138].

Activation of $Os_7(CO)_{21}$ by Me_3NO in CH_2Cl_2/MeCN affords the labile cluster $Os_7(CO)_{19}(MeCN)_2$. This MeCN-substituted cluster reacts with dppf to produce $Os_7(CO)_{17}(\mu_4\text{-}\eta^2\text{-}CO)(MeCN)(dppf)$ in moderate yield. The molecular structure was shown to consist of an unprecedented Os_7 core with a 'spiked' osmium atom appended at the equatorial plane of the capped trigonal bipyramid. CV studies reveal the existence of some electronic/electrostatic interactions between the cluster core and the ferrocene center [139].

2.5. Group 9 clusters

The reactivity of several cobalt carbonyl compounds under vacuum conditions is reported. The equilibrium decomposition of $Co_2(CO)_8$ to $Co_4(CO)_{12}$ was explored, and the formation of $HCo_3(CO)_9$ was observed to be promoted under semi-stoichiometric oxo conditions (i.e., low pCO or in the absence of CO) [140]. New Co_3 clusters containing face-capping arene ligands have been prepared. Catalytic hydrogenation of the alkene side chain in the *facial* alkenylbenzene ligands in $(CpCo)_3[\mu_3\text{-}C_6H_5(CR)(CHR')]$ affords the corresponding reduction products $(CpCo)_3[\mu_3\text{-}C_6H_5(CHR)(CH_2R')]$. X-ray structural analyses on two derivatives reveal that the μ_3-phenyl rings show a small but significant Kekulé-type distortion. All products exhibit a hindered rotation of the μ_3-arene groups on the top of the $(CpCo)_3$ clusters, as confirmed by NMR spectroscopy [141]. The ligand diphenyl-2-thienylphosphine reacts with $MeCCo_3(CO)_9$ to give $MeCCo_3(CO)_8[PPh_2(C_4H_3S)]$ and $MeCCo_3(CO)_7[PPh_2(C_4H_3S)]_2$. The two products have been characterized in solution and by X-ray methods in the case of the latter cluster [142]. Treatment of propargyl trichloroacetate with $Co_2(CO)_8$ gives the pentacobalt compound $[Co_2(CO)_6][HCCCO_2CCo_3(CO)_9]$ and $EtCCo_3(CO)_9$. The X-ray structure of the Co_5 complex consists of a Co_3 triangle and an alkyne-substituted Co_2 moiety [143]. The thioarsine $AsPh_2(SPh)$ reacts with $Co_2(CO)_8$ to furnish the tricobalt cluster $Co_3(\mu_3\text{-}S)(\mu\text{-}ASPh_2)(CO)_6(AsPh_3)$, whose molecular structure has been determined and discussed relative to other Co_3 clusters [144]. The tagging of carbohydrates with the cluster moiety $CCo_3(CO)_9$ is reported. These compounds are prepared from $[+COCCo_3(CO)_9]$ or from the reaction of $Co_2(CO)_8$ with a suitable 1,1,1-tribromomethyl sugar derivative. The X-ray structure of one product and the 2-D ^1H- and ^{13}C-NMR data for all new clusters are discussed. These carbohydrate-cluster compounds show reversible redox activity in organic and aqueous solution [145]. A report describing the use of subtractively normalized interfacial FTIR spectroscopy (SNIFTIRS) in the electrochemical study of $[Co_3(CO)_9C]_2$ has appeared. The ability of this technique to investigate ECE transformations is discussed [146]. The use of $(CO)_9Co_3(\mu_3\text{-}CCOOH)$ as a template in the construction of novel polynuclear materials has been published. When this cluster is allowed to react with metal trifluoroacetates, cluster-stabilized analogues of known organic carboxylates are produced in good yields [147]. Room temperature fragmentation of bis-(diphenylphosphino)dimethylhydrazine is observed when treated with $PhCCo_3(CO)_9$. The major product isolated and structurally characterized was $PhCCo_3(CO)_8[Ph_2PP(O)Ph_2]$ [148]. The reaction of ethyl diazoacetate with a mix-

ture of $ClCCo_3(CO)_9$ and $AlCl_3$ leads to several clusters, of which $HCCo_3(CO)_9$, $EtO_2CCCo_3(CO)_9$, $EtO_2CCH_2CCo_3(CO)_9$, and $[Co_3(CO)_9(\mu_3\text{-}CCHCO_2Et)]_2$ have been isolated by column chromatography. The identity of the last cluster was ascertained by X-ray crystallography [149]. Nitrosobenzene reacts with $[Cp^*Rh(\mu\text{-}Cl)(\mu\text{-}S^iPr)_2RhCp^*]^+$ to afford the incomplete cubane cluster $[(Cp^*Rh)_3(\mu\text{-}Cl)_2(\mu_3\text{-}S)(\mu\text{-}S^iPr)]^+$, which has been fully characterized in solution and by X-ray diffraction analysis [150].

A review dealing with comparative solid-state and solution NMR structural and dynamic behavior of tetra- and higher-nuclearity Group 9 metal clusters has appeared [151]. The X-ray structure of $Co_4(CO)_{12}$ has been determined at 120 K and redetermined at r.t. At low temperature, the CO groups for both disordered components have been resolved, providing a more accurate structure for $Co_4(CO)_{12}$. The observed solid-state disorder at ambient temperature indicates that the Co_4 tetrahedral rotates inside a relatively rigid ligand polytope [152]. The use of quantum theory of atoms in molecules (QTAM) in the determination of charge density in $Co_4(CO)_{12}$ and $Co_4(CO)_{11}(PPh_3)$ is described [153]. The tetracobalt cluster $Co_4(CO)_{10}(\mu\text{-}CO)[\mu_4\text{-}\eta\text{:}\eta^3\text{-}CC(CH_2OCH_2)CCH_2]$ is the unexpected product from the reaction between $Co_2(CO)_8$ and $HC_2CH_2OCH_2C_2H$. X-ray diffraction analysis proves that the 'yne' fragment of the diyne ligand is bonded to a $Co_2(CO)_6$ moiety with the C≡C vector being almost perpendicular to the Co–Co vector [154]. The synthesis and X-ray structure of $Co_4(CO)_{10}(\mu\text{-}P,N\text{-}PPh_2py)$ have been published. This Co_4 cluster is prepared from the thermolysis of $Co_2(CO)_8$ with PPh_2py [155]. $Rh_4(CO)_{12}$ functions as a catalyst precursor for the synthesis of 2-(dimethylphenylsilylmethyl)alkenal from 2-propynylamine and two equivalents of Me_2PhSiH under CO. The mechanism for this reaction is discussed [156]. Detailed kinetic data for the regioselective catalytic hydroformylation of styrene to (±)-2-phenylpropanal and 3-phenylpropanal using $Rh_4(CO)_{12}$ have been published. Quantitative high-pressure in-situ IR measurements made under isobaric and isothermal conditions have allowed for the observation of the acyl intermediates (±)-$PhCH(Me)CORh(CO)_4$ and $PhCH_2CH_2CORh(CO)_4$. Reaction mechanisms and selected spectral data are presented [157]. The hydroformylation of cyclohexene to cyclohexanecarboxaldehyde was studied by using $Rh_4(CO)_{12}$ as the catalyst precursor. Cluster fragmentation to mononuclear rhodium species was verified by high-pressure in-situ IR measurements. No evidence was obtained for a catalytic binuclear elimination sequence, but rather aldehyde formation was shown to arise from the hydrogenolysis of the $RCORh(CO)_4$ intermediate with molecular H_2 as the rate-determining step [158]. The reactivity of $M_4(\mu\text{-}pyS_2)_2(1,5\text{-}COD)_4$ (where M = Rh, Ir) with $TlPF_6$ has been investigated. New $TlRh_4$ clusters were isolated and characterized in solution and by electrochemical and MO methods [159]. Treatment of the hydrogensulfido-bridged complexes $Cp^*MCl(\mu\text{-}SH)_2MClCp^*$ (where M = Rh, Ir) with $CuCl_2{\cdot}2H_2O$ gives the Rh_4 cluster $[(Cp^*Rh)_4(\mu_3\text{-}S)_2(\mu_4\text{-}S_3)][CuCl_2]_2$ and the Ir_3 cluster $[(Cp^*Ir)_3(\mu_3\text{-}S_2)_3(CuCl_2)][CuCl_2]$. The molecular structures of these two clusters were solved by X-ray crystallography [160]. Protonation of $[Cp^*Ir(CN)_3]^-$ leads to the two-dimensional organometallic solid $(H_2O)[Cp^*Ir(CN)_3]{\cdot}$acetone, which contains 14 Å diameter channels of $Ir_4C_8N_8O_4$

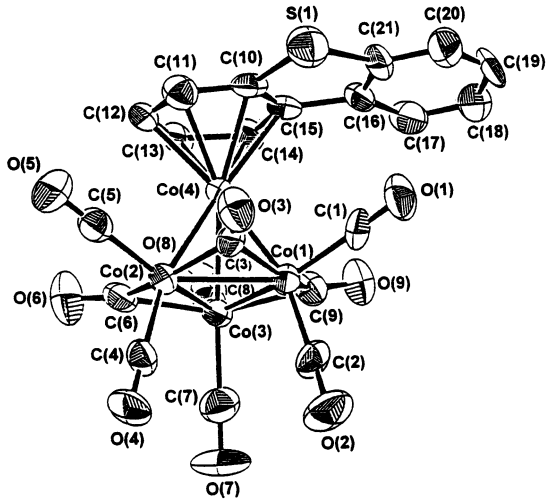

Fig. 8. X-Ray structure of (η^6-DBT)$Co_4(CO)_9$. Reprinted with permission from Organometallics. Copyright 1999 American Chemical Society.

atoms [161]. The reaction of $Co_4(CO)_{12}$ with dibenzothiophene and benzothiophene is reported. In the case of the former thiol compound, the cluster complex (η^6-DBT)$Co_4(CO)_9$, which contains one η^6-coordinated arene ring to a single cobalt center, was isolated and characterized by X-ray analysis (Fig. 8). Desulfurization was observed when (η^6-DBT)$Co_4(CO)_9$ was treated with $Cr(CO)_3(MeCN)_3$, giving (η^6-benzene)$Co_4(CO)_9$. This same product cluster was obtained from the reaction between $Co_4(CO)_{12}$ and benzothiophene [162].

Sigma bond metathesis of a B–H bond in $Cp^*_2Rh_2B_3H_6Cl$ with the Co–Co bond in $Co_2(CO)_8$ furnishes the pentanuclear cluster $Cp^*_2Rh_2Co_3(CO)_8B_3HCl$ in 30% yield. This 82-electron cluster possesses a structure based on a rectangular faced-capped trigonal prismatic cluster. A scheme illustrating the cluster build-up pathway and the X-ray structure of the product are discussed [163]. The rhodium-catalyzed cyclic carbonylation of 2-phenylethynylbenzamide under water-gas shift conditions is presented. The catalyst precursor employed was $Rh_6(CO)_{16}$. The utility of this reaction in the construction of a wide variety of heterocycles is discussed [164]. The synthesis and solid-state structure of $[Ir_{11}(CO)_{23}]^{3-}$ have been published. The Ir_{11} product is obtained from the reaction between $[Ir_{10}(CO)_{21}]^{2-}$ and $[Ir(CO)_4]^-$ in refluxing MeCN. The Ir_{11} cluster exhibits a metallic core having D_{3h} symmetry, with three faced-fused octahedral, all of which share a common edge [165].

2.6. Group 10 clusters

A report on the 'ship-in-bottle' synthesis of platinum carbonyl clusters in titania- and zircona-modified mesoporous channels of FSM-16 has appeared. Treatment of

H_2PtCl_6 with CO and H_2O at 323 K in modified FSM-16 gives the clusters $[Pt_3(CO)_6]_n^{2-}$ (where $n = 4–6$). The conversion of these clusters into Pt nanoparticles has also been examined [166]. The linear triplatinum complexes linear-$[Pt_3(\mu\text{-dpmp})_2(RNC)_2]^{2+}$ react with $[NO][BF_4]$ to give the unprecedented nitrosyl-bridged double-A-frame clusters $[Pt_3(\mu\text{-dpmp})_2(\mu\text{-NO})_2(RNC)_2]^{2+}$. The X-ray structure of the mesityl derivative has been solved, and extended Hückel MO calculations confirm the presence of a small HOMO-LUMO gap [167]. Depending upon the reaction conditions, either $Pd_2(\mu\text{-SO}_2)(\mu\text{-dba})(PBz_3)_2$ or $Pd_3(\mu\text{-SO}_2)_3(PBz_3)_3$ may be isolated from the reaction of $Pd_2(dba)_3$ with added PBz_3 and SO_2. The Pd_2 complex reacts with CO to furnish a mixture of the triangular clusters $Pd_3(\mu\text{-CO})_2(\mu\text{-SO}_2)(PBz_3)_3$ and $Pd_3(\mu\text{-CO})(\mu\text{-SO}_2)_2(PBz_3)_3$. When the same Pd_2 complex is allowed to react with CN^{t}Bu, only $Pd_3(\mu\text{-SO}_2)_2(CN^tBu)_2(PBz_3)_3$ was observed. The X-ray structures of $Pd_3(\mu\text{-CO})_2(\mu\text{-SO}_2)(PBz_3)_3$ and the isonitrile-substituted cluster have been determined, with differences between these 42- and 44-electron clusters discussed relative to other structurally characterized examples [168]. The unusual tetraplatinum cluster [*cis*-$Pt(C_6F_5)_2(PPh_3)(\mu_3\text{-}1\kappa C^{\alpha}\text{:}2\kappa C^{\beta}\text{:}3\kappa N\text{–}C_2C_5N\text{-}2)$][$Pt_3(C_6F_5)_2(\mu_3\text{-}3\kappa C^{\alpha}\text{:}\eta^2_{\alpha,\beta}\text{:}2\kappa N\text{–}CH{=}CHC_5H_5N\text{-}2)(PPh_3)_2$] has been synthesized from *trans*-PtH(C≡C-2-pyridyl) and *cis*-$Pt(C_6F_5)_2(THF)_2$. The molecular structure of this Pt_4 complex is best described as a formal zwitterionic cationic Pt_3 cluster-substituted alkynyl platinate complex [169]. The synthesis, spectroscopic data, and solid-state structure of $Pd_4(\mu\text{-SO}_2)_2(\mu_3\text{-S})(CO)(PBz_3)_3$ have been published. This tetrahedral cluster is obtained from $Pd_2(\mu\text{-dba})(\mu\text{-SO}_2)(PBz_3)_2$ and COS [170]. The molecular structures of $[H_xNi_{12}(CO)_{21}][Me_4N]_{4-x}\cdot S$ (where $x = 1$, S = acetone; $x = 2$, S = THF) are reported. Both anions exhibit similar X-ray structures, and their structures have also been examined by solid-state ^{1}H-MAS and ^{13}C-CP/MAS-NMR spectroscopy. The observed VT-NMR behavior is discussed relative to the X-ray structures [171]. The clusters $[Pt_{19}(CO)_{21}(NO)]^{3-}$ and $[Pt_{38}(CO)_{44}]^{2-}$ have been synthesized and structurally characterized. The role of nitrosyl bending in the former cluster by an intramolecular electron transfer and its subsequent conversion to the Pt_{38} cluster are discussed. $[Pt_{38}(CO)_{44}]^{2-}$ serves as an example of a cluster complex that exhibits the largest known homometallic core exclusively stabilized by CO ligands and the smallest polyhedron for which an inner octahedron is completely surrounded by a second shell of metal atoms [172]. The electron-sink behavior of the carbonylnickel clusters $[Ni_{32}C_6(CO)_{36}]^{6-}$ and $[Ni_{38}C_6(CO)_{42}]^{6-}$ is discussed. The X-ray structure of the Ni_{32} cluster is included, and the results of protonation and electrochemical studies are presented [173]. New Ni/Pt carbonyl clusters with a tetrahedron of nickel atoms have been prepared. Treatment of $[Ni_6(CO)_{12}]^{2-}$ with K_2PtCl_6 gives six products, of which $[Ni_{36}Pt_4(CO)_{45}]^{6-}$ and $[Ni_{37}Pt_4(CO)_{46}]^{6-}$ have been structurally characterized [174].

2.7. Group 11 clusters

The luminescence behavior of the copper acetylide complexes $[Cu_3(\mu\text{-dppm})_3(\mu_3\text{-}\eta^1\text{-C}{\equiv}CR)]^{2+}$, $[Cu_3(\mu\text{-dppm})_3(\mu_3\text{-}\eta^1\text{-C}{\equiv}CR)_2]^{+}$, and $Cu_4(PPh_3)_4(\mu_3\text{-}\eta^1\text{-C}{\equiv}CR)_4$ has been examined. Each cluster was shown to exhibit rich photoluminescent chemistry.

Also presented are the emission data and excited-state reducing properties of $[Cu_3(\mu\text{-dppm})_3(\mu_3\text{-}\eta^1\text{-}C{\equiv}CR)_2]^+$, which support the intervention of a $Cu^ICu^ICu^{II}$ species when the photolysis is conducted in the presence of a pyridinium electron acceptor [175]. The synthesis and X-ray structure of $[Ag_3(C_2^tBu)_2]_n$, which was obtained from the reaction between $AgBF_4$ and $[Ag(C_2^tBu)]_n$, have been published [176]. A review on the luminescent chemistry exhibited by polynuclear Group 11 and other metal acetylide complexes has appeared [177]. The mixed Group 11 clusters $[M\{Au(2\text{-}CH_2\text{-}6\text{-}RC_5H_3N)(PPh_3)\}_2]^+$ (where M = Cu, Ag) have been prepared from $Au(2\text{-}CH_2\text{-}6\text{-}RC_5H_3N)(PPh_3)$. In the case of the $AgAu_2$ derivative, X-ray analysis reveals the presence of short interactions between the gold and silver centers [178].

3. Heteronuclear clusters

3.1. Trinuclear clusters

The early–late trinuclear complexes $Cp(acac)Ti(\mu_3\text{-}S)_2[M(diolefin)]_2$ (where M = Rh, Ir; diolefin = 1,5-COD, tetrafluorobenzobarrelene) have been synthesized from $Cp_2Ti(SH)_2$ and M(acac)(diolefin). The complex reaction sequence leading to the TiM_2 products is discussed, and the replacement of the diolefin and the acac ligands by added ligands is described. Two X-ray structures accompany this report [179].

The cobalt dithiolene complex $CpCo(S_2C_6H_4)$ reacts with $Mo(CO)_3(py)_3$ to afford the linear cluster $[CpCo(S_2C_6H_4)]_2Mo(CO)_2$, which contains a central $Mo(CO)_2$ moiety bridged by two cobaltadithiolene rings. The X-ray structure was solved, and the electrochemical behavior was investigated by cyclic voltammetric measurements. An EEC mechanism was observed, with the cluster dianion decomposing to the radical anion and unknown fragmentation products [180]. A kinetic study on the migration of the $W(CO)_5$ moiety on the disulfide ligand in $[CpFe(CO)_2]_2(\mu_3\text{-}S_2)W(CO)_5$ has appeared. VT ^{1}H-NMR data have allowed for the construction of a working mechanism that involves the oxidative addition of the $W(CO)_5$ moiety across the S–S bond. The X-ray structures of $[CpFe(CO)_2]_2(\mu_3\text{-}S_2)W(CO)_5$ and $Cp_2Fe_2(CO)_3(\mu\text{-}CO)(\mu_3\text{-}S)W(CO)_5$ are presented [181]. The synthesis and reactivity of the tetrahedral clusters $(\eta^5\text{-}RC_5H_4)(CO)_2MFe_2H(\mu_3\text{-}E)(CO)_6$ (where M = Mo, W; E = S, Se; R = various groups) have been published. All new compounds were fully characterized in solution by the normal methods, in addition to ^{77}Se-NMR spectroscopy in the case of the selenium-capped clusters. The molecular structures of $(\eta^5\text{-}MeCOC_5H_4)(CO)_2WFe_2H(\mu_3\text{-}E)(CO)_6$ (where E = S and Se) and $(\eta^5\text{-}MeCOC_5H_4)(CO)_2MFeCo(\mu_3\text{-}S)(CO)_5(PPh_3)$ (where M = Mo and W) have been crystallographically determined [182]. The mixed-metal clusters RCpM-CpWFe$(CO)_7(\mu_3\text{-}S)$ (RCp = MeCp, Cp; M = Mo, W) have been synthesized from the tetrahedral cluster $CpWFeCo(CO)_7(\mu_3\text{-}S)$ and its reaction with $RCpM(CO)_3Cl$. The X-ray structure of $CpWMeCpWFe(CO)_7(\mu_3\text{-}S)$ has been solved, and the two independent cluster molecules in the unit cell were shown to be enantiomers of each other [183]. When $[Cp^*WS_3]^-$ is allowed to react with two equivalents of CuBr, the

octanuclear cluster $[Cp^*WS_3Cu]_4$ was isolated in high yield. Carrying out the same reaction in the presence of excess PPh_3 furnishes the trinuclear cluster $Cp^*WS_3Cu_2Br(PPh_3)_2$. Both clusters were structurally characterized by X-ray methods. The former cluster consists of a W_4Cu_4 core having approximate S_4 symmetry, while the latter cluster exhibits an incomplete cubane core [184]. The synthesis and NMR analysis of $[\{Cp_2Mo(\mu_2\text{-}H)_2\}_2Ag]^+$ and $[\{Cp_2W(\mu_2\text{-}H)_2\}_2Ag]^+$ have been published. Through the use of ^1H- and $^1H\{^{109}Ag\}$-NMR measurements, details concerning the structure, bonding, and hydride exchange behavior have been elucidated [185]. The methoxynitrido-substituted cluster $Ru_3(CO)_9(\mu_3\text{-}CO)(\mu_3\text{-}NOMe)$ reacts with the hydride compound $CpMo(CO)_3H$ at r.t. to ultimately give $Ru_2Mo(\mu\text{-}H)(CO)_8Cp(\mu_3\text{-}NOMe)$ and $Ru_2Mo(\mu\text{-}H)(CO)_8Cp(\mu_3\text{-}NH)$. Both Ru_2Mo clusters consist of a triangular metallic core that is capped by a μ_3-N ligand. When $Ru_3(CO)_9(\mu_3\text{-}CO)(\mu_3\text{-}NOMe)$ is allowed to react with $[CpMo(CO)_3]_2Hg$, the pentanuclear cluster $Ru_3(CO)_{10}(\mu\text{-}NH_2)(\mu_3\text{-}Hg)[CpMo(CO)_3]$ was isolated as the major product [186]. The trinuclear cluster $[Cp^*Ru(CO)_2]_2W(\mu_3\text{-}S)(\mu_2\text{-}S)_2(=S)$ (Fig. 9) and the isomeric tetranuclear clusters $[Cp^*Ru(CO)_2]_2[W(\mu_3\text{-}S)_2(\mu_2\text{-}S)_2][W(CO)_5]$ and $[Cp^*Ru(CO)_2]_2[W(\mu_3\text{-}S)_3(=S)][W(CO)_5]$ were obtained from the reaction between $Cp^*Ru_2S_4$ and two equivalents of $W(CO)_3(MeCN)_3$. Use of one equivalent of $W(CO)_3(MeCN)_3$ produces $[Cp^*Ru(CO)_2]_2W(\mu_2\text{-}S)_4$, which is an isomer of the other Ru_2W cluster. These two trinuclear clusters are converted to the tetranuclear clusters by reaction with $W(CO)_3(MeCN)_3$ and CO. Mechanistic schemes showing the Ru_2W transformations to the Ru_2W_2 clusters are presented [187].

The 33-electron complex $Cp_2Mo_2(CO)_4(\mu\text{-}PPh_2)$, which is a reactive binuclear radical, reacts with $Re_2(CO)_{10}$ under continuous photolysis to give the trinuclear complex $Mo_2ReCp(\mu\text{-}C_5H_4)(\mu\text{-}H)(\mu\text{-}PPh_2)(CO)_8$. The solid-state structure has been solved by X-ray diffraction analysis, which verified the formal C–H bond activation of one Cp ring at the rhenium center [188]. The borole-containing complex $[(\mu\text{-}C_4H_4BPh)Re(CO)_3]^-$ reacts with $HgCl_2$ to produce the Re_2Hg complex $[(\mu\text{-}C_4H_4BPh)Re(CO)_3]_2Hg$, which exhibits a linear metal chain. Use of the borole

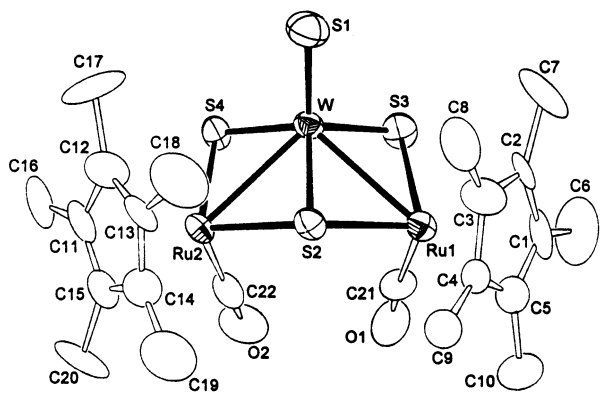

Fig. 9. X-Ray structure of $[Cp^*Ru(CO)_2]_2W(\mu_3\text{-}S)(\mu_2\text{-}S)_2(=S)$. Reprinted with permission from Organometallics. Copyright 1999 American Chemical Society.

complex $[(\mu\text{-}C_4H_4BPh)Fe(CO)_2H]^-$ with *trans*-$[PtBr_2(4\text{-}Mepy)_2]$ gives the corresponding Fe_2Pt cluster *trans*-$Pt[(\mu\text{-}C_4H_4BPh)Fe(CO)_2H]_2(4\text{-}Mepy)_2$. The X-ray structures of both clusters accompany this report [189]. The use of *cis*-$[Mn(CO)_4(2\text{-}S\text{–}C_4H_3S)_2]^-$ as a metallo chelating ligand in the construction of $(CO)_4Mn(\mu\text{-}2\text{-}C_4H_3S)_2Ni(\mu\text{-}2\text{-}C_4H_3S)_2Mn(CO)_4$ has been reported. The electronic properties of this Mn_2Ni cluster are discussed relative to the Ni–Mn distances and the square planar nickel center. Three X-ray structures are included in this report [190]. The reactivity of the vinylidene complex $Cp(CO)_2MnPt(\mu\text{-}C{=}CHPh)(\eta^2\text{-}dppm)$ with $Fe_2(CO)_9$ has been explored. The mixed-metal clusters $CpMnFePt(\mu_3\text{-}C{=}CHPh)(\mu\text{-}dppm)(CO)_5$ and $(\eta^2\text{-}dppm)PtFe_3(\mu_4\text{-}C{=}CHPh)(CO)_9$ have been isolated and characterized in solution and by X-ray crystallography in the case of the MnFePt cluster, which is shown to exist in two isomeric forms. Also reported is the X-ray structure of $CpMnFePt(\mu_3\text{-}C{=}CHPh)(CO)_6[\eta^1\text{-}Ph_2PCH_2P(O)Ph_2]$ [191].

The X-ray structure of $(CO)_5(PPh_3)_2FePt_2(\mu_3\text{-}Se)$ has been found to consist of an $FePt_2Se$ butterfly core, with each platinum atom bearing one CO and one PPh_3 group [192]. The preparation and X-ray structures of $(CpCo)_2[Fe(CO(CNC_6H_4Me\text{-}4)(PPh_3)](\mu_3\text{-}S)(\mu_3\text{-}CO)$ have been published [193]. The synthesis, redox chemistry, and X-ray structure of $Fe_2(CO)_6(\mu_3\text{-}S)_2Ni(dppf)$ have been presented. The arachno polyhedral core was confirmed by X-ray analysis. The cyclic voltammetric data are discussed relative to the results obtained from extended Hückel MO calculations [194]. The tetrahedrane cluster $FeCo_2(CO)_9(\mu_3\text{-}S)$ has been allowed to react with the diphosphine ligand bpcd to produce $FeCo_2(CO)_7(bpcd)(\mu_3\text{-}S)$. The substitution occurs readily under thermolysis conditions and by Me_3NO activation. X-ray structural analysis reveals that the bpcd ligand is bound to a single cobalt center in a chelating fashion. The cyclic voltammetric data indicate that the observed $0/1^-$ and $1^-/2^-$ redox couples are bpcd centered and not associated with the population of an antibonding metal-based orbital consisting of Fe–Co and Co–Co bonds [195]. Metallosite selectivity in $CyPH_2$ substitution reactions in $HMCo_3(CO)_{12}$ (where M = Fe, Ru) and cluster degradation of $HMCo_3(CO)_{11}(CyPH_2)$ are reported. The corresponding μ_3-phosphinidene-capped clusters $MCo_2(CO)_9(\mu_3\text{-}PCy)$ are obtained from $HMCo_3(CO)_{11}(CyPH_2)$ via the intermediate clusters $MCo_4(\mu_4\text{-}PCy)(\mu\text{-}CO)_2(CO)_{11}$. In this reaction the cluster transformation is accelerated by the addition of Me_3NO. This report represents a rare example where a cluster fragmentation reaction proceeds by the following nuclearity sequence $4 \rightarrow 5 \rightarrow 3$. The X-ray structures of $RuCo_4(\mu_4\text{-}PCy)(\mu\text{-}CO)_2(CO)_{11}$ and $RuCo_2(\mu_3\text{-}PCy)(CO)_9$ (Fig. 10) have been solved and employed in the formulation of a working reaction sequence [196].

The polynuclear complex $Co_2[\mu\text{-}Me_3SiC{\equiv}CC_2C{\equiv}C\{Ru(PPh_3)_2Cp\}](CO)_4(dppm)$ has been synthesized and examined for electronic interactions between the cobalt and ruthenium centers. The electronic structure of this complex has been modeled by using DFT, ZINDO, and ELF calculations [197]. The crystal structure of the linked cluster $RuCo_2(CO)_9[\mu_3\text{-}\eta^2\text{-}HC_2CH_2OC_6H_4OCH_2C_2H\text{-}\eta^2\text{-}\mu_3]RuCo_2(CO)_9$ has been published [198]. The synthesis of new $RuIr_2$ clusters is described. The hydrogensulfido-bridged complex $Cp^*IrCl(\mu\text{-}SH)_2IrClCp^*$ serves as the starting material from which $(Cp^*Ir)_2(\mu_3\text{-}S)_2RuCl_2(PPh_3)$ and $[(Cp^*Ir)_2(\mu_3\text{-}S)_2RuCl(P\text{–}P)]^+$

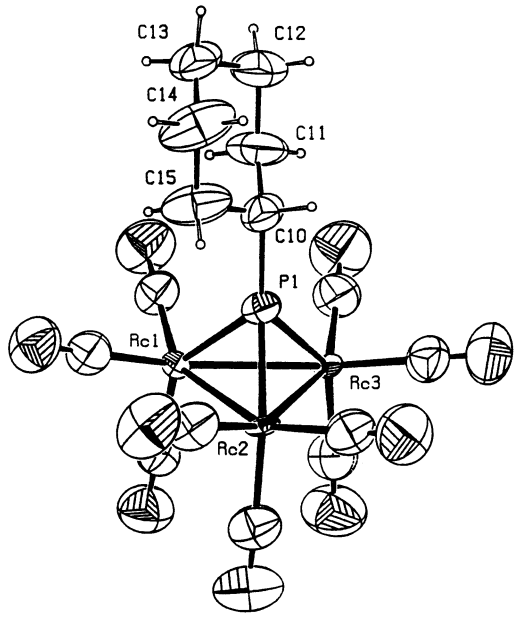

Fig. 10. X-Ray structure of $RuCo_2(\mu_3\text{-}PCy)(CO)_9$. Reprinted with permission from Organometallics. Copyright 1999 American Chemical Society.

(where P–P = dppe, depe) may be synthesized. The ancillary chlorine ligand(s) in these clusters may be converted into a hydride group(s) upon treatment with $NaBH_4$. Five X-ray structures are included in this report [199].

The new cluster $PtRu_2(CO)_5(\mu\text{-}CO)(\mu\text{-}dppm)_2$ has been isolated from the reaction between $[Pt(dppm)_2][Cl]_2$ and $[HRu(CO)_4]^-$. This multistep reaction proceeds via the intermediate dinuclear species $[HPtRu(CO)_3(\mu\text{-}dppm)_2]^+$, which then reacts with additional $[HRu(CO)_4]^-$ to afford the $PtRu_2$ product cluster. The X-ray structure of $PtRu_2(CO)_5(\mu\text{-}CO)(\mu\text{-}dppm)_2$ consists of a $PtRu_2$ triangle where the two Pt–Ru edges are each bridged by a dppm ligand. While a μ_2-CO group is observed by X-ray analysis, CO scrambling about the cluster polyhedron is still rapid on the NMR time scale down to -90°C [200]. The synthesis of soluble carbosilane dendrimers terminated by $AuFe_2$ and $AuFe_3$ carbonyl cluster units is described [201]. A cluster possessing a facially coordinated COT ligand has been prepared from $CpNiCo_3(CO)_9$ and COT. The product of this reaction, $Co_2Ni(CO)_6(\mu_3\text{-}\eta^2\text{:}\eta^3\text{:}\eta^3\text{-}C_8H_8)$, was characterized in solution and by X-ray diffraction analysis. The identity of the metal atoms could not be unequivocally established from the diffraction data. Each metal contains a terminal CO group and each M–M vector is bridged by a CO ligand. In solution all six CO groups are rapidly scrambling about the cluster polyhedron in a 'merry-go-round' sequence, as determined by VT ^{13}C-NMR measurements [202]. The synthesis of new Co_2Pt, Co_2Pd, and $MoPd_2$ mixed-metal clusters using the P–N–P assembling ligands $(Ph_2P)_2NH$ and $(Ph_2P)_2NMe$ is discussed. Isolated and structurally characterized was $Co_2Pd(\mu_3\text{-}$

CO)$(CO)_6$[μ-$(Ph_2P)_2$NH] [203]. [Pt(dppm)$_2$][Cl]$_2$ reacts with $[Ir(CO)_4]^-$ and dppm to produce the new cluster $PtIr_2(CO)_2$(μ-CO)(μ-dppm)$_3$, which is shown to contain a $PtIr_2$ triangular core with each edge bridged by a dppm ligand and in which only the platinum center is coordinatively unsaturated. CO equilibration about the cluster polyhedron gives rise to different isomers of this cluster, all of which have been studied by spectroscopic means and by X-ray methods. The X-ray structures of $PtIr_2(CO)_2$(μ-CO)(μ-dppm)$_3$, $[PtIr_2(CO)_3$(μ-dppm)$_2]^+$, and $PtIr_2(CO)_4$(μ-CO)(μ-dppm)$_2$ are reported, and a detailed picture of the cluster growth mechanism operative in this genre of cluster is discussed [204]. The reactivity of palladium(II) complexes containing the orthometallated C,C-chelating ligand C_6H_4-2-$PPh_2C(H)COCH_2PPh_3$ in cluster buildup reactions has been examined. The trinuclear cluster complex $[Pd_2Hg(\mu\text{-}Cl)_2\{C_6H_4\text{-}2\text{-}PPh_2C(H)COC(H)PPh_3\}]^{2+}$ was prepared from $Hg(OAc)_2$ and $[Pd(\mu\text{-}Cl)\{C_6H_4\text{-}2\text{-}PPh_2C(H)COC(H)PPh_3\}]_2^{2+}$. The molecular structure of this compound was ascertained by X-ray crystallography [205].

3.2. Tetranuclear clusters

The reaction of the thiotitanate complex $[(CpTiS)_2(\mu\text{-}S)_2]^{2-}$ with $[Cp^*RuCl]_4$, $[M(1,5\text{-}COD)(\mu\text{-}Cl)]_2$ (where M = Rh, Ir), and $[Cu(PPh_3)Cl]_4$ affords the early-late cubane-type sulfido clusters $(CpTi)_2(Cp^*Ru)_2(\mu_3\text{-}S)_4$, $(CpTi)_2[M(1,5\text{-}COD)]_2(\mu_3\text{-}S)_4$, and $(CpTi)_2[Cu(PPh_3)]_2(\mu_3\text{-}S)_4$, respectively. The X-ray structures of the Ti_2Rh_2 and Ti_2Cu_2 derivatives have been solved [206]. A general route to the cluster compounds $CpTi(\mu_3\text{-}S)_3M_3$(diolefin)$_3$ (where M = Rh, Ir; diolefin = 1,5-COD, nbd, tfbb) has been published. Treatment of these clusters with CO gives the 62-electron carbonyl clusters $CpTi(\mu_3\text{-}S)_3M_3(CO)_6$. The reactivity of the iridium species with phosphine and phosphite ligands is also discussed. The X-ray structure of $CpTi(\mu_3\text{-}S)_3Ir_3$(μ-CO)$(CO)_3$[$P(OMe)_3$] consists of an iridium triangle that exhibits an interaction between the tetrahedral iridium atom and the titanium center. Isotopic exchange with added ^{13}CO was found to be rapid at r.t., and the observed CO fluxionality in these clusters has been studied by VT ^{13}C-NMR measurements [207]. The use of $CpTi(\mu_3\text{-}S)_3$[Rh(diolefin)]$_3$ as a catalyst in the hydroformylation of 1-hexene and styrene is described. These reactions were conducted under mild conditions with a 96% conversion to aldehydes and 77% regioselectivity for the linear aldehyde in the hydroformylation of 1-hexene. The regioselectivity to 2-phenylpropanal is reported to be 80% for styrene hydroformylation. High-pressure NMR studies have allowed for the observation of pertinent catalytic intermediates, all of which appear to maintain the $TiRh_3$ nuclearity [208].

Cluster syntheses using $RCp_2Fe_2S_4$ [where RCp = Cp*, 1,3-$C_5H_3(SiMe_3)_2$] have been documented. When these sulfide templates are allowed to react with $M(CO)_3(MeCN)_3$ or $M(CO)_6$ (where M = Mo, W), the tetranuclear tetrathiolate clusters $[RCpFe(CO)]_2[M(\mu_3\text{-}S)_2(\mu\text{-}S)_2][M(CO)_4]$ may be isolated as the major products. $[Cp^*Ru(MeCN)_3]^+$ reacts with $RCp_2Fe_2S_4$ to produce $[(Cp^*)_2(RCp)_2Fe_2Ru_2S_4]^+$. The X-ray structures of three clusters accompany this report [209]. The heterobimetallic complex $(OC)_3Co(\mu\text{-}As_2)MoCp(CO)_2$ reacts with

$Cr(CO)_5(THF)$ to give the new cluster $(OC)_3Co[\mu\text{-}As_2\{Cr(CO)_5\}_2]MoCp(CO)_2$, whose structure was verified by X-ray diffraction analysis. Also presented are the syntheses and structures of the trimetallic clusters $M_2M'(\mu_3\text{-}As)Cp_3(CO)_6$ (where M, M′ = Cr, Mo, W) [210]. The cubane cluster $(\eta^6\text{-}p\text{-}^iPrC_6H_4Me)_4Ru_4Mo_4O_{16}$ gives the new tetrametal cluster $(\eta^6\text{-}p\text{-}^iPrC_6H_4Me)_2Ru_2Mo_2O_6(OMe)_4$ when treated with *p*-hydroquinone in methanol. X-ray analysis reveals that the Ru_2Mo_2 cluster consists of two $Mo_2Ru(OMe)_3$ half-cubes that are fused together to form a chair-like structure [211]. Treatment of $Fe_2(CO)_6(\mu\text{-}SSe)$ with $Cp_2Mo_2(CO)_4$ at r.t. gives the new isomeric clusters *cis*- and *trans*-$Cp_2Mo_2Fe_2(CO)_8(\mu_3\text{-}S)(\mu_3\text{-}Se)$. These same products were obtained from the thermolysis of $Fe_3(CO)_9(\mu_3\text{-}S)(\mu_3\text{-}Se)$ and $Cp_2Mo_2(CO)_6$. The structural identity of these isomers was established by X-ray crystallography [212]. Ligand substitution in $Cp_2W_2Ir_2(CO)_{10}$ by $P(OMe)_3$ leads to $Cp_2W_2Ir_2(\mu_3\text{-}CO)_3(CO)_6[P(OMe)_3]$ and $Cp_2W_2Ir_2(\mu_3\text{-}CO)_3(CO)_5[P(OMe)_3]_2$. X-ray structural studies on the former cluster reveal that the $P(OMe)_3$ ligand is bound to an iridium center and to an iridium center and a tungsten center in the case of the latter cluster. The solution ^{13}C- and ^{31}P-NMR spectra are discussed relative to the X-ray structures [213]. The alkyne-bridged complexes $Mo_2(\mu\text{-}HC_2Ph)(CO)_4[\eta^5\text{-}C_5H_4C(O)R]_2$ (where R = Me, OEt, Ph) react with $Co_2(CO)_8$ in refluxing toluene to yield the new butterfly clusters $Co_2Mo_2(\mu_4\text{-}HC_2Ph)(\mu\text{-}CO)_4(CO)_4[\eta^5\text{-}C_5H_4C(O)R]_2$. Full characterization by solution methods is discussed, and the X-ray structure of $Co_2Mo_2(\mu_4\text{-}HC_2Ph)(\mu\text{-}CO)_4(CO)_4[\eta^5\text{-}C_5H_4C(O)Me]_2$ is presented [214]. Deprotonation of a proton bridging a B–H–Ru edge in $HRu_3WCp(CO)_{11}BH$ gives $[HRu_3WCp(CO)_{11}B]^-$, which is fluxional in solution. This anionic cluster reacts with $Au(PPh_3)Cl$ to give the aurated cluster $HRu_3WCp(CO)_{11}B(AuPPh_3)$ in high yield. X-ray structural analysis reveals that the gold(I) phosphine moiety takes the place of the B–Ru bridging proton in the starting cluster. Anion functionalization using ClAu(dppf)AuCl is also reported [215]. Isomer distribution and ligand fluxionality in $CpWIr_3(\mu\text{-}CO)_3(CO)_{8-n}(PR_3)_n$ (where $n = 1, 2$; R = Ph, OMe) have been examined by VT ^{31}P- and ^{13}C-NMR spectroscopy, COSY spectra, and X-ray structural studies. The proposed mechanisms for carbonyl fluxionality have been verified by carrying out EXSY-NMR measurements [216]. The reaction of $Cp_2W_2Ir_2(CO)_{10}$ with PPh_3 and PMe_3 proceed readily at r.t. to give mono- and disubstituted clusters. All of the products show ligand fluxionality in solution at ambient temperature, resolvable at low temperature into the constituent interconverting isomers. The solid-state structure of $Cp_2W_2Ir_2(\mu\text{-}CO)_3(CO)_6(PPh_3)$ was determined, and the results are discussed relative to the solution NMR data. Included in this discussion is the use of ^1H-^{31}P-^{13}C-NMR correlation data, designed to elucidate P–C coupling networks involving the phosphorus and CO ligands [217]. The reactions of dppm and dppe with $Cp_2W_2Ir_2(CO)_{10}$ have been studied by a variety of NMR methods. The site selectivity associated with these reactions and the fluxional nature of the phosphine-substituted products are discussed [218]. The diynyl complex $Cp^*W(O)_2(C{\equiv}CC{\equiv}CPh)$ reacts with $H_2Os_3(CO)_{10}$ to furnish the cluster $Os_3(CO)_{10}(\mu\text{-}H)[\mu\text{-}\eta^3\text{-}C(=CHPh)C{\equiv}CW(O)_2Cp^*]$. ^1H-NMR data indicate that three isomers of this cluster are present in solution, of which two isomers have been structurally characterized (Fig. 11). Reactivity studies with this Os_3W cluster

have afforded the clusters $Os_3(CO)_{10}(\mu\text{-}\sigma{:}\eta^2\text{-}C{\equiv}CCHCHPh)$ and $Cp^*W(O)_2\text{-}Os_3(CO)_9(\mu\text{-}\sigma{:}\eta^2\text{-}C{\equiv}CCHCHPh)$ [219].

The mixed-metal hydroxy cubane cluster $[Re(CO)_3]_3(PtMe_3)(OH)_4$ has been isolated from the reaction between $[Re_3(CO)_9(OH)_4]^-$ and $(PtMe_3I)_4$. The X-ray structure and NMR data for this cluster are presented and discussed [220]. An example of a novel inorganic benzene ring coordinated to a Re_2Co_2 cluster has appeared. Treatment of $Cp^*_2Re_2B_4H_8$ with $Co_2(CO)_8$ leads to $(Cp^*Re)_2[\mu\text{-}\eta^6{:}\eta^6\text{-}B_4H_4Co_2(CO)_5]$ (Fig. 12), whose X-ray structure shows a 6π electron $[B_4H_4Co_2(CO)_5]^{6-}$ ring that is capped by two Cp*Re groups. The geometry of this cluster is discussed with respect to PSEP theory [221].

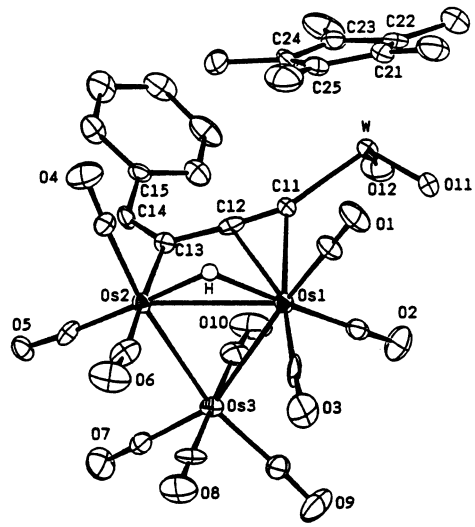

Fig. 11. X-Ray structure of $Os_3(CO)_{10}(\mu\text{-}H)[\mu\text{-}\eta^3\text{-}C(=CHPh)C{\equiv}CW(O)_2Cp^*]$. Reprinted with permission from Organometallics. Copyright 1999 American Chemical Society.

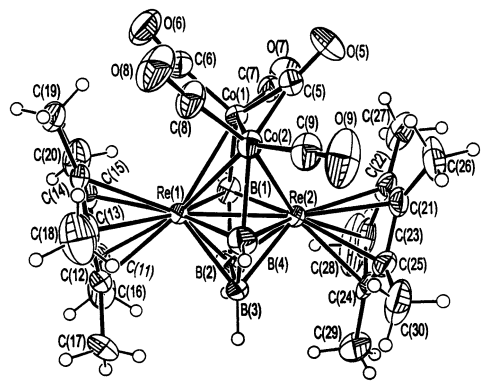

Fig. 12. X-Ray structure of $(Cp^*Re)_2[\mu\text{-}\eta^6{:}\eta^6\text{-}B_4H_4Co_2(CO)_5]$. Reprinted with permission from Journal of American Chemical Society. Copyright 1999 American Chemical Society.

Alkyne-carbide coupling on a WOs_3 cluster is reported. 4-ethynyl toluene reacts with $Cp^*WOs_3(\mu_4\text{-}C)(\mu\text{-}H)(CO)_{11}$ to yield the alkylidyne cluster $Cp^*WOs_3(\mu_3\text{-}CCHCHTol)(CO)_{11}$, which contains a *trans* CH=CHTol ligand. Use of 3-phenyl-1-propyne gives the alkenyl carbido cluster $Cp^*WOs_3(\mu_4\text{-}C)(CHCHCH_2Ph)(CO)_{10}$ and the alkylidyne species $Cp^*WOs_3[\mu_3\text{-}CC(CH_2Ph)(CH_2)](CO)_{10}$. Mechanisms accounting for the formation of these clusters are presented, and the X-ray structures of the latter two clusters are fully discussed [222]. Good to excellent yields of $CpWIr_3(CO)_{11-n}(CNR)_n$ (where $n = 1–3$; R = mesityl, ^{t}Bu) were obtained when $CpWIr_3(CO)_{11}$ was allowed to react with CNR. The fluxional properties of the ancillary CO ligands were investigated by ^{13}C-NMR spectroscopy. An all-terminal ligand geometry was found in the X-ray structure of $CpWIr_3(CO)_9(CNmesityl)_2$ [223]. A paper describing the synthesis and structural characterization of $[Fe_3(\mu_3\text{-}O)(\mu_3\text{-}AuPPh_3)(\mu\text{-}CO)_3(CO)_6]^-$, $[Au_6(\mu_3\text{-}S)_2(PPh_3)_6][Fe_3(\mu_3\text{-}S)(\mu\text{-}AuPPh_3)(CO)_9]_2$, and $[Au_6(\mu_3\text{-}S)_2(PPh_3)_6][Fe_5(\mu_3\text{-}S)_2(CO)_{14}]$ has appeared. The latter two clusters represent new examples of ionic solids assembled from cluster–cations and cluster–anions [224]. Hydride addition to $Ru_3(\mu\text{-}H)(\mu_3\text{-}C_2H)(CO)_3$ using K-Selectride, followed by treatment with $AuCl(PPh_3)$, gives the three clusters $AuRu_3(\mu\text{-}H)(\mu_3\text{-}C_2H)(CO)_9(PPh_3)$, $Au_2Ru_3(\mu_3\text{-}C{=}CH_2)(CO)_9(PPh_3)_2$, and $Ru_3(\mu\text{-}H)[\mu_3\text{-}CHCH(OH)](CO)_8(PPh_3)$. The solid-state structure of each product was crystallographically determined [225]. The fixation and spontaneous dehydrogenation of methanol on a Ru_3Ir cluster are described. The anionic cluster $[Ru_3Ir(CO)_{13}]^-$ reacts with methanol via O–H bond activation to give $[HRu_3Ir(CO)_{12}(OMe)]^-$, which upon prolonged reaction loses formaldehyde to produce $[H_2Ru_3Ir(CO)_{12}]^{2-}$. The 62-electron monoanionic cluster exhibits a butterfly Ru_3Ir skeleton, while the dianionic cluster possesses a tetrahedral Ru_3Ir core, as verified by X-ray diffraction studies. A working mechanism illustrating the methanol activation process and the changes associated in the cluster core as a function of methanol activation are discussed [226]. The reaction between the tetrahedral cluster $[Ru_3Ir(CO)_{13}]^-$ and internal alkynes affords $[Ru_3Ir(CO)_{11}(RC_2R')]^-$. The resulting butterfly clusters contain a $\mu_4\text{-}\eta^2$-coordinated alkyne ligand. These clusters fragment to $[Ru_2Ir(CO)_9(RC_2R')]^-$ under CO pressure. The protonation chemistry of these anions is discussed, and the X-ray structures of seven clusters have been determined [227]. The synthesis, crystal structure, and solution characterization of $Ru_2Ir_2H(CO)_{12}Cl$ have been published. This new cluster is obtained from the reaction between $Ru_2(CO)_6Cl_4$ and $[Ir(CO)_4][Na]$. A butterfly arrangement of metal atoms was found, with three terminal CO groups on each metal atom and a hydride-bridged Ir–Ir vector. Use of $[Ir(CO)_4][K]$ leads to the trinuclear cluster $Ru_3(\mu\text{-}Cl)_2(CO)_8(PPhMe_2)_2$, after ligand substitution with $PPhMe_2$ [228]. Treatment of $Os_3(CO)_{12}$ with $[Ir(CO)_4]^-$ gives the tetrahedral cluster $[Os_3Ir(CO)_{13}]^-$. X-ray analysis reveals that one of the CO groups bridges an Os–Ir vector. Protonation of this cluster gives $HOs_3Ir(CO)_{13}$, whereas reaction with H_2 affords $[H_2Os_3Ir(CO)_{12}]^-$. The catalytic activity of $[Os_3Ir(CO)_{13}]^-$ in the carbonylation of methanol was examined. When MeI is employed as cocatalyst, catalytic turnover numbers up to 1800 were observed [229]. The synthesis, characterization, and X-ray crystal structures of $Os_3Rh(\mu\text{-}CO)(CO)_9(\mu_4\text{-}\eta^2\text{-}$

$PhC_2Ph)(\mu_2\text{-}\eta^1\text{:}\eta^2\text{-}PhC_2PhH)$, $Os_6Rh(\mu\text{-}H)_9(CO)_{18}$, $Os_6Rh(\mu\text{-}H)_7(\mu\text{-}CO)(CO)_{18}$, and $[Os_6Rh(\mu\text{-}H)_2(CO)_{20}]^{2-}$ are reported. The observed structures are discussed relative to the valence electron count at each cluster [230]. Phosphine, phosphite, arsine, and stibine ligand substitution in $[H_2Ru_3Ir(CO)_{12}]^-$ has been investigated, with site selectivity being discussed as a function of the nature of the incoming ligand and the extent of ligand substitution [231]. The three clusters $Os_3Rh(\mu\text{-}H)_2(\mu\text{-}CO)(CO)_9Cp^*$, $Os_3Rh(\mu\text{-}CO)_2(CO)_9Cp^*$, and $Os_3Rh_2(\mu\text{-}H)(\mu\text{-}CO)_2(CO)_8Cp^*(\mu_2\text{-}\eta^5\text{:}\eta^1\text{-}CH_2C_5Me_4)$ have been isolated from the reaction between $[Os_3(CO)_{11}H]^-$ and $[Cp^*Rh(MeCN)_3]^+$. Solid-state vacuum thermolysis of $Os_3Rh(\mu\text{-}CO)_2(CO)_9Cp^*$ gives $Os_3Rh(\mu\text{-}H)_2(\mu\text{-}CO)(CO)_9Cp^*$. When the coupling reaction is carried out with $[Cp^*Rh(dppe)Cl]^+$ in place of $[Cp^*Rh(MeCN)_3]^+$, only $Os_3Rh(\mu_3\text{-}H)(\mu\text{-}Cl)(\mu\text{-}CO)(CO)_9Cp^*$ was obtained. Each product was fully characterized in solution and by X-ray crystallography in the case of three clusters [232].

New Os/Hg clusters have been synthesized by using organomercurial starting materials. The activated cluster $Os_3(CO)_{10}(MeCN)_2$ reacts with $PhHgS(C_5H_4N)$ to give two new clusters *cis*-$Os(CO)_4[Os_3(CO)_{10}(\mu\text{-}\eta^2\text{-}SC_5H_4N)(\mu\text{-}Hg)]_2$ and $[Os_3(CO)_{10}(\mu\text{-}\eta^2\text{-}SC_5H_4N)]_2(\mu_4\text{-}Hg)$. Use of PhHg(mbt) gives $[Os_3(CO)_{10}(\mu\text{-}\eta^2\text{-}mbt)]_2(\mu_4\text{-}Hg)$ and $Os_3(CO)_{10}(\mu\text{-}\eta^2\text{-}mbt)[\mu\text{-}\eta^2\text{-}Hg(mbt)]$. The reactivity of other polynuclear clusters with several different organomercurial complexes is presented [233]. Collman's reagent reacts with $Ag_2(dppm)_2(NO_3)_2$ and $Au_2(dppm)_2Cl_2$ to produce $[Ag_3\{\mu\text{-}Fe(CO)_4\}(dppm)_3]^+$ and $[Au_3\{\mu\text{-}Fe(CO)_4\}(dppm)_2]^+$, respectively. X-ray analysis has unambiguously shown that the $Fe(CO)_4$ moiety is triply bridging in the Ag_3 cluster and doubly bridging in the Au_3 cluster. Degradation of $[Ag_{13}\{\mu_3\text{-}Fe(CO)_4\}_8]^{3-}$ with dppm gives the aforementioned Ag_3 cluster [234].

3.3. Pentanuclear clusters

$Rh_4(CO)_{12}$ reacts with $Pt(PPh_3)_3$ to produce the pentanuclear cluster $Rh_2Pt_3(\mu\text{-}CO)_5(CO)_4(PPh_3)_3$ and the tetanuclear cluster $Rh_2Pt_2(\mu\text{-}CO)_3(CO)_4(PPh_3)_3$. Both products were characterized in solution by various NMR methods [^{13}C, ^{31}P, (^{31}P-^{31}P) COSY, and (^{13}C-^{103}Rh) and (^{31}P-^{103}Rh) heteronuclear multiple quantum coherence (HMQC)]. The NMR data have confirmed the butterfly structure in the Rh_2Pt_2 cluster. X-ray diffraction analysis revealed that the 72-electron Rh_2Pt_3 cluster conforms to Wade's rules, exhibiting a trigonal bipyramidal polyhedron. The CO migration pathways in $Rh_2Pt_2(\mu\text{-}CO)_3(CO)_4(PPh_3)_3$ were elucidated by a combination of EXSY and 1D VT NMR measurements. A scheme involving an independent localized exchange about the hinge rhodium atoms and interchange of the bridging and semi-bridging CO groups about the Pt–Rh vectors is presented and discussed [235]. The tungsten oxo acetylide complex $Cp^*W(O)_2CCPh$ reacts with $Ru_4(CO)_{13}(\mu_3\text{-}PNR_2)$ (where $R = {}^iPr$, Cy) to furnish the oxo-bridged clusters $Cp^*W(\mu\text{-}O)Ru_4(CO)_9(\mu\text{-}CO)[\mu_3\text{-}\eta^2\text{-}P(O)NR_2](\mu_4\text{-}\eta^2\text{-}CCPh)$ and $Cp^*W(\mu\text{-}O)_2Ru_4(CO)_{10}(\mu_3\text{-}PNR_2)(\mu_4\text{-}\eta^2\text{-}CCPh)$. The X-ray structural data for these two products are presented, and the protonation reactivity in these clusters is discussed [236]. Tail-to-tail carbon–carbon bond coupling of acetylides in chalcogen-bridged FeW clusters have been observed. The new clusters $W_2Fe_3Cp^*_2(CO)_6(\mu_3\text{-}E)_2[\mu_4\text{-}$

CC(Ph)C(Ph)C] (where E = S, Se, Te) have been synthesized from $Fe_3(CO)_9(\mu_3\text{-}E)_2$ and $Cp^*W(CO)_3(C{\equiv}CPh)$. All products were characterized in solution by IR and NMR spectroscopy (^1H, ^{13}C, ^{77}Se, ^{125}Te). Included in this report is the X-ray structure of the $W_2Fe_3S_2$ derivative [237]. The stepwise construction of Ru_2PtW and Ru_2Pt_2W clusters is observed in the reaction between $[Cp'Ru(CO)_2]_2[W(\mu\text{-}S)_4]$ (where $Cp' = Cp^*$, C_5Me_4Et) and $PtMe_2$(1,5-COD). The two products isolated and structurally characterized were $[(C_5Me_4Et)Ru(CO)_2]_2[W(\mu_3\text{-}S)_2(\mu\text{-}S)_2](PtMe_2)$ and $[Cp^*Ru(CO)_2]_2[W(\mu_3\text{-}S)_4](PtMe_2)_2$ [238]. Cluster build-up reactions using an ionic coupling route are described. $[Os_4H_4(CO)_{11}]^{2-}$, formed by the reduction of $Os_4H_4(CO)_{12}$ with potassium benzophenone ketyl, reacts with $[Cp^*Rh(MeCN)_3]^+$ to yield a number of penta- and hexanuclear mixed–metal clusters. The crystal and molecular structures of $Os_4Rh(\mu\text{-}H)_3(MeC{=}NH)(CO)_{11}Cp^*$, $Os_4Rh(\mu\text{-}H)_2(CO)_{13}Cp^*$, and $Os_4Rh_2(\mu\text{-}H)_2(CO)_{11}Cp_2^*$ were determined and their geometries discussed. $Os_4Rh(\mu\text{-}H)_3(MeC{=}NH)(CO)_{11}Cp^*$ contains the uncommon MeC=NH moiety that is coordinated to an edge-bridged tetrahedral metal core, while the other Os_4Rh cluster possesses an Os_4 tetrahedral core that exhibits an edge-bridging Rh atom. The sole hexanuclear cluster exhibits a bicapped tetrahedron, where the two rhodium atoms face cap two faces of the Os_4 tetrahedron [239]. An ionic coupling reaction was employed in the synthesis of the new cluster $Os_3CoRu(CO)_{13}Cp$ and the known clusters $HOs_3Ru(CO)_{11}Cp$ and $Os_3Ru_2(CO)_{11}Cp_2$. A trigonal bipyramidal polyhedron having approximate C_s symmetry was found for the Os_3CoRu cluster by X-ray crystallography [240]. The transformation of ethylene to ethylidyne on an $IrRu_4$ cluster is reported. $HIrRu_4(CO)_{13}$ reacts with ethylene in hexane at 90°C to give $H_3IrRu_3(CO)_{12}$ and $HIrRu_4(CO)_{15}(\mu_4\text{-}CCH_3)$. X-ray structural analysis confirms the coordination of the ethylidyne ligand to the four ruthenium atoms [241].

3.4. Hexanuclear clusters

$Co_2(CO)_8$ complexation across the alkyne bonds in $M(C{\equiv}CC{\equiv}CR)(CO)_3Cp$ [where M = Mo, W; R = H, $CpFe(CO)_2$] affords the bis-cluster complexes $Cp(CO)_8Co_2M(\mu_3\text{-}C)C{\equiv}CCo_2M(CO)_8Cp$. The use of extended Hückel and density functional theory calculations in understanding the observed $M_3C_4M_3$ structure is discussed. Three X-ray structures have been solved, and the structural data are discussed relative to related clusters [242]. Mixed-metal gold phosphines have been synthesized. This report includes synthetic and X-ray structural data on $Au_4Co_2(CO)_7(PPh_3)_3$, $Re_2Au_2(CO)_7$(dppf), and $[AuCo(CO)_4]_2$(*cis*-$Ph_2PCH{=}CHPPh_2$). The intramolecular aurophilic interactions present in some of these clusters are discussed [243]. The ability of semi-rigid polyene ligands to direct the shapes of metal clusters has been demonstrated. Treatment of $Pt_2Ru_4(CO)_{18}$ with *o*-bis(phenylethynyl)benzene gives $Pt_2Ru_4(CO)_{14}[\mu_5\text{-}C_6H_4(C_2Ph)_2]$, which displays an unexpected 'raft' arrangement for the six metal atoms. The X-ray structure of this 88-electron cluster is presented, and the influence of this bisalkyne in controlling the 'raft' geometry, which is uncommon for this electron count, is discussed [244]. New osmium-palladium clusters containing a bridging 2-

(diphenylphosphino)pyridine ligand are described. The reaction between $Os_5C(CO)_{14}(Ph_2Ppy)$ with $Pd(MeCN)_2Cl_2$ gives $Os_5PdC(CO)_{14}(\mu\text{-}Cl)Cl(\mu\text{-}Ph_2Ppy)$, which is thermally unstable in refluxing $CHCl_3$ and decomposes to give $[Os_4C(CO)_{10}(\mu\text{-}Cl)(\mu\text{-}Ph_2Ppy)(\mu_4\text{-}Pd)\{Os_4C(CO)_{12}(\mu\text{-}Cl)\}]$ and $[Os_4(\mu_5\text{-}C)(CO)_{12}(\mu\text{-}Cl)]_2(\mu\text{-}Pd_2Cl_2)$. The original Os_5Pd cluster reacts with I_2 to produce $Os_5PdC(CO)_{14}(\mu\text{-}Cl)I(\mu\text{-}Ph_2Ppy)$ and $[Os_4(\mu_5\text{-}C)(CO)_{12}(\mu\text{-}I)]_2(\mu\text{-}Pd_2I_2)$. All of these products have been characterized in solution and by X-ray crystallography [245]. A relativistic density functional study on $[Fe_3Pt_3(CO)_{15}]^{n-}$ (where $n = 0, 1, 2$) has been conducted and the data published. The optimized geometries agree well with the available experimental structures, especially with respect to Pt–Pt and Pt–Fe bond distances. The trend observed in the calculated bond distances is consistent with experimental data and supports a Pt–Pt antibonding interaction in the HOMO. Additional insight into the electronic structure of these clusters is revealed by the calculated binding energies, ionization potentials, and electron affinities [246]. Polynuclear Fe–Co clusters derived from butadiynyl and butadiynediyl iron complexes have been synthesized and characterized by solution and X-ray methods. Examples of cluster framework reorganization and valence isomerization of the C_4H linkage are presented [247]. A report on the skeletal rearrangements and X-ray structures of $Au_2Ru_4(CO)_{12}(\mu_4\text{-}PCF_3)(PMe_3)_2$ and $Au_2Ru_4(CO)_{12}(\mu_3\text{-}PCF_3)_2(PPh_3)_2$ has appeared [248]. Treatment of $[Os_4H_4(CO)_{11}]^{2-}$, $[Os_{10}C(CO)_{24}]^{2-}$, and $[Ru_{10}C(CO)_{24}]^{2-}$ with $Au_2(dppe)Cl_2$ in the presence of excess $TlPF_6$ furnishes the new clusters $Os_4H_4(CO)_{11}(Au_2dppe)$, $Os_{10}C(CO)_{24}(Au_2dppe)$, and $Ru_{10}C(CO)_{24}(Au_2dppe)$, all of which were isolated in high yield. The X-ray structure of the Os_4Au_2 and the $Ru_{10}Au_2$ clusters were determined, and the novel modes of coordination exhibited by the bidentate gold fragments are discussed [249]. An unusual intramolecular metallalactone reaction has been observed in the reaction between $Ru_3(\mu\text{-}H)[\mu_3\text{-}C_2CPh_2(OH)](CO)_9$ and $AuCl(PPh_3)$ in the presence of K-Selectride. The isolated product, $Au_3Ru_3[\mu_3\text{-}\eta^1\text{:}\eta^1\text{:}\eta^1\text{:}\eta^2\text{-}CCHCPh_2OC(O)](CO)_8(PPh_3)_3$, is believed to have formed by the intramolecular attack of the alkoxide ion on an adjacent CO ligand. The molecular structure of this Au_3Ru_3 cluster was confirmed by X-ray crystallography [250].

3.5. Higher nuclearity clusters

Aggregation of the tungsten sulfido complex $[Cp^*WS_3]^-$ with AgCN leads to the cyanide-bridged helical polymer $[(Cp^*WS_3)_2Ag_3(CN)]_\infty$ and the cyclic cluster $(Cp^*WS_3Ag)_4$. Both complexes were characterized in solution and their molecular structures were determined by X-ray methods [251]. The synthesis and X-ray structure of $[\{Pt_2Ag_8(C{\equiv}C^tBu)_8(OClO_3)_2(acetone)\}(O_2ClO_2)_2]_n$ have been reported. This complex was obtained from the reaction between $Pt_2Ag_4(C{\equiv}C^tBu)_8$ and $AgClO_4$ [252]. Carbosilane dendrimers functionalized with $AuFe_3$ clusters have been prepared and characterized in solution [253]. The platinum–copper acetylide complex of stoichiometry $PtCu_2(C{\equiv}CPh)_4$ was shown by X-ray diffraction analysis to consist of discrete trimers of the hexanuclear octahedral unit $[Pt_2Cu_4(C{\equiv}CPh)_8]_3$. Strong axial Pt···Pt interactions give rise to rich photoluminescent behavior in both

the solid state and fluid solution [254]. The synthesis of large Au–Pd–Ni carbonyl clusters is reported. Data on the preparation, structural bonding analysis, and physical properties of $[Au_6Pd_6(Pd_{6-x}Ni_x)Ni_{20}(CO)_{44}]^{6-}$ are described. This cluster represents the first crystallographically determined example of a high-nuclearity trimetal cluster possessing only CO ligands [255].

Appendix A

Ar-BIAN	bis(arylimino)-acenaphthene
bpy	2,2′-bipyridine
bpm	2,2′-bipyrimidine
bzim	1-benzylimidazole
COD	1,5-cyclooctadiene
COT	cyclooctatraene
Cp	cyclopentadienyl
Cp*	pentamethylcyclopentadienyl
Cy	cyclohexyl
dba	dibenzylideneacetone
DBT	dibenzothiophene
depe	bis(diethylphosphino)ethane
dmpm	bis(dimethylphosphino)methane
dpmp	$(Ph_2PCH_2)_2PPh$
dpp	2,3-bis(2-pyridyl)pyrazine
dppa	1,2-bis(diphenylphosphino)acetylene
dppb	1,4-bis(diphenylphosphino)butane
dppe	1,2-bis(diphenylphosphino)ethane
dppf	1,1′-bis(diphenylphosphino)ferrocene
dppm	bis(diphenylphosphino)methane
dppp	1,3-bis(diphenylphosphino)propane
dpq	2,3-bis(2-pyridyl)-5,6-dimethylquinoxaline
Fc	ferrocenyl
ind	indenyl
MAS	magic angle spinning
mbt	mercaptobenzothiazole
MeCp	methylcyclopentadienyl
nbd	norbornadiene
PPN	bis(triphenylphosphine)iminium
py	pyridine
pyz	pyrazine
tpa	tris(2-pyridylmethyl)amine
Tol	tolyl
xy	2,6-Me_2phenyl

References

[1] C.D. Abernethy, Diss. Abstr. Sect. B 59 (1999) 4098 [DANQ29462].
[2] I.S. Zavarine, Diss. Abstr. Sect. B 59 (1999) 4108 [DA9900412].
[3] R.W. Eveland, Diss. Abstr. Sect. B 59 (1999) 6316 [DA9913790].
[4] B.R. Bergman, Diss. Abstr. Sect. B 59 (1999) 5844 [DA9914169].
[5] P.J. Martellaro, Diss. Abstr. Sect. B 60 (1999) 642 [DA9919764].
[6] M.D. Westmeyer, Diss. Abstr. Sect. B 59 (1999) 4807 [DA9904620].
[7] H. Shan, Diss. Abstr. Sect. B 60 (1999) 1604 [DA9925335].
[8] K.T. McBride, Diss. Abstr. Sect. B 59 (1999) 3434 [DA9841746].
[9] A.J. Marzec, Diss. Abstr. Sect. B 59 (1999) 4105 [DA9902491].
[10] G.J. Spivak, Diss. Abstr. Sect. B 59 (1999) 3436 [DANQ28522].
[11] N.T. Tran, Diss. Abstr. Sect. B 60 (1999) 182 [DA9904206].
[12] C.D. Abernethy, F. Bottomley, R.W. Day, A. Decken, D.A. Summers, R.C. Thompson, Organometallics 18 (1999) 870.
[13] L.Y. Goh, W. Chen, R.C.S. Wong, J. Chem. Soc., Chem. Commun. (1999) 1481.
[14] L.Y. Goh, W. Chen, R.C.S. Wong, Organometallics 18 (1999) 306.
[15] B. Rink, M. Brorson, I.J. Scowen, Organometallics 18 (1999) 2309.
[16] F. Ossola, F. Benetollo, J. Organomet. Chem. 580 (1999) 56.
[17] A.S. Weller, M. Shang, T.P. Fehlner, Organometallics 18 (1999) 853.
[18] M. Shieh, H.-S. Chen, H.-Y. Yang, C.-H. Ueng, Angew. Chem., Int. Ed. 38 (1999) 1252.
[19] R. Sevvel, T.-W. Tseng, K.-L. Lu, J. Organomet. Chem. 582 (1999) 160.
[20] A.C. Hillier, A. Sella, M.R.J. Elsegood, J. Organomet. Chem. 588 (1999) 200.
[21] M. Bergamo, T. Beringhelli, G. D'Alfonso, P. Mercandelli, M. Moret, A. Sironi, Angew. Chem., Int. Ed. 38 (1999) 3486.
[22] T. Beringhelli, G. D'Alfonso, M. Panigati, F. Porta, P. Mercandelli, M. Moret, A. Sironi, J. Am. Chem. Soc. 121 (1999) 2307.
[23] C. Roveda, E. Cariati, E. Lucenti, D. Roberto, J. Organomet. Chem. 580 (1999) 117.
[24] I. Shimoyama, T. Hachiya, M. Mizuguchi, T. Nakamura, M. Kaihara, T. Ikariya, J. Organomet. Chem. 584 (1999) 197.
[25] J. Liu, E.P. Boyd, S.G. Shore, Acta Cryst. C55 (1999) 29.
[26] L.J. Farrugia, A.L. Gillon, D. Braga, F. Grepioni, Organometallics 8 (1999) 5022.
[27] D.C.D. Butler, D.J. Cole-Hamilton, Inorg. Chem. Commun. 2 (1999) 305.
[28] D. Berger, W. Imhof, J. Chem. Soc., Chem. Commun. (1999) 1457.
[29] N. Chatani, T. Morimoto, A. Kamitani, Y. Fukumoto, S. Murai, J. Organomet. Chem. 579 (1999) 177.
[30] T. Morimoto, N. Chatani, S. Murai, J. Am. Chem. Soc. 121 (1999) 1758.
[31] N. Chatani, Y. Ie, F. Kakiuhi, S. Murai, J. Am. Chem. Soc. 121 (1999) 8645.
[32] F. Kakiuchi, T. Sato, M. Yamauchi, N. Chatani, S. Murai, Chem. Lett. (1999) 19.
[33] T.E. Müller, A.-K. Pleier, J. Chem. Soc., Dalton Trans. (1999) 583.
[34] T. Mitsudo, N. Suzuki, T. Kobayashi, T. Kondo, J. Mol. Catal. A. Chem. 137 (1999) 253.
[35] F. Ragaini, A. Ghitti, S. Cenini, Organometallics 18 (1999) 4925.
[36] F. Ragaini, S. Cenini, S. Tollari, G. Tummolillo, R. Beltrami, Organometallics 18 (1999) 928.
[37] X. Dai, N. Kano, M. Kako, Y. Nakadaira, Chem. Lett. (1999) 717.
[38] P. Nombel, Y. Hatanaka, S. Shimada, M. Tanaka, Chem. Lett. (1999) 159.
[39] K. Matsubara, A. Inagaki, M. Tanaka, H. Suzuki, J. Am. Chem. Soc. 121 (1999) 7421.
[40] G. Lavigne, Eur. J. Inorg. Chem. (1999) 917.
[41] M. Faure, L. Maurette, B. Donnadieu, G. Lavigne, Angew. Chem., Int. Ed. 38 (1999) 518.
[42] M. Tokunaga, M. Eckert, Y. Wakatsuki, Angew. Chem., Int. Ed. 38 (1999) 3222.
[43] L. Maurette, B. Donnadieu, G. Lavigne, Angew. Chem., Int. Ed. 38 (1999) 3707.
[44] R.W. Eveland, C.C. Raymond, D.F. Shriver, Organometallics 18 (1999) 534.
[45] S.N. Konchenko, A.V. Virovets, S.A. Apenina, S.V. Tkachev, Inorg. Chem. Commun. 2 (1999) 555.

[46] A.J. Carty, G. Hogarth, G.D. Enright, J.W. Steed, D. Georganopoulou, J. Chem. Soc., Chem. Commun. (1999) 1499.
[47] D. Cauzzi, C. Graiff, G. Predieri, A. Tiripicchio, C. Vignali, J. Chem. Soc., Dalton Trans. (1999) 237.
[48] D. Cauzzi, C. Graiff, C. Massera, G. Predieri, A. Tiripicchio, D. Acquotti, J. Chem. Soc., Dalton Trans. (1999) 3515.
[49] N. Choi, G. Conole, M. Kessler, J.D. King, M.J. Mays, M. McPartlin, G.E. Pateman, G.A. Solan, J. Chem. Soc., Dalton Trans. (1999) 3941.
[50] C. Decker, W. Henderson, B.K. Nicholson, J. Chem. Soc., Dalton Trans. (1999) 3507.
[51] H.G. Ang, S.G. Ang, S. Du, B.H. Sow, X. Wu, J. Chem. Soc., Dalton Trans. (1999) 2799.
[52] H.-G. Ang, S.-G. Ang, S. Du, J. Organomet. Chem. 590 (1999) 1.
[53] D.J. Ellis, P.J. Dyson, D.G. Parker, T. Welton, J. Mol. Catal. A: Chem. 150 (1999) 71.
[54] B. Fontal, M. Reyes, T. Suárez, F. Bellandi, J.C. Díaz, J. Mol. Catal. A: Chem. 149 (1999) 75.
[55] B. Fontal, M. Reyes, T. Suárez, F. Bellandi, N. Ruiz, J. Mol. Catal. A: Chem. 149 (1999) 87.
[56] L.T. Byrne, J.P. Hos, G.A. Koutsantonis, B.W. Skelton, A.H. White, J. Organomet. Chem. 592 (1999) 95.
[57] M.I. Bruce, O. Kühl, B.W. Skelton, A.H. White, Aust. J. Chem. 52 (1999) 705.
[58] M.I. Bruce, P.A. Humphrey, B.W. Skelton, A.H. White, K. Costuas, J.-F. Halet, J. Chem. Soc., Dalton Trans. (1999) 479.
[59] S.E. Kabir, M. Karim, K.M. Abdul Malik, T.A. Siddiquee, Inorg. Chem. Commun. 2 (1999) 128.
[60] I. Godefroy, H. Stoeckli-Evans, G. Süss-Fink, Inorg. Chem. Commun. 2 (1999) 247.
[61] M.I. Bruce, B.W. Skelton, A.H. White, N.N. Zaitseva, Inorg. Chem. Commun. 2 (1999) 17.
[62] N.J. Goodwin, W. Henderson, B.K. Nicholson, J. Fawcett, D.R. Russell, J. Chem. Soc., Dalton Trans. (1999) 1785.
[63] S.G. Bott, J.C. Wang, M.G. Richmond, J. Chem. Crystallogr. 29 (1999) 587.
[64] G. Gervasio, R. Giordano, D. Marabello, E. Sappa, J. Organomet. Chem. 588 (1999) 83.
[65] W.K. Leong, Y. Liu, J. Organomet. Chem. 584 (1999) 174.
[66] E.C. Constable, C.E. Housecroft, A.G. Schneider, J. Organomet. Chem. 573 (1999) 101.
[67] N.E. Leadbeater, J. Organomet. Chem. 573 (1999) 211.
[68] P.J. Dyson, A.K. Hearley, B.F.G. Johnson, J.S. McIndoe, P.R.R. Langridge-Smith, Inorg. Chem. Commun. 2 (1999) 591.
[69] W.K. Leong, Y. Liu, Organometallics 18 (1999) 800.
[70] M. Faure, M. Jahncke, A. Neels, H. Stoeckli-Evans, G. Süss-Fink, Polyhedron 18 (1999) 2679.
[71] M.S. Morton, J.P. Selegue, J. Organomet. Chem. 578 (1999) 133.
[72] H. Braunschweig, C. Kollann, M. Koster, U. Englert, M. Müller, Eur. J. Inorg. Chem. (1999) 2277.
[73] W.K. Leong, M.W. Lum, Acta Cryst. C55 (1999) 881.
[74] J. Zachara, A. Zimniak, Acta Cryst. C55 (1999) 58.
[75] A. Zimniak, J. Zachara, M. Olejnik, J. Organomet. Chem. 589 (1999) 239.
[76] M.I. Bruce, B.W. Skelton, A.H. White, N.N. Zaitseva, Aust. J. Chem. 52 (1999) 413.
[77] A.J. Poë, C. Moreno, Organometallics 18 (1999) 5518.
[78] D.D. Ellis, A. Franken, F.G.A. Stone, Organometallics 18 (1999) 2362.
[79] R.D. Adams, U.H.F. Bunz, W. Fu, G. Roidl, J. Organomet. Chem. 578 (1999) 55.
[80] E. Sappa, J. Organomet. Chem. 573 (1999) 139.
[81] M.I. Bruce, B.W. Skelton, A.H. White, N.N. Zaitseva, J. Chem. Soc., Dalton Trans. (1999) 1445.
[82] C.S.-W. Lau, W.-T. Wong, J. Chem. Soc., Dalton Trans. (1999) 607.
[83] C.S.-W. Lau, W.-T. Wong, J. Organomet. Chem. 589 (1999) 198.
[84] C.S.-W. Lau, W.-T. Wong, J. Chem. Soc., Dalton Trans. (1999) 2511.
[85] W.-Y. Yeh, M.-A. Hsu, S.-M. Peng, G.-H. Lee, Organometallics 18 (1999) 880.
[86] T. Ito, T. Hamaguchi, H. Nagino, T. Yamaguchi, H. Kido, I.S. Zavarine, T. Richmond, J. Washington, C.P. Kubiak, J. Am. Chem. Soc. 121 (1999) 4625.
[87] K. Ota, H. Sasaki, T. Matsui, T. Hamaguchi, T. Yamaguchi, T. Ito, H. Kido, C.P. Kubiak, Inorg. Chem. 38 (1999) 4070.

[88] J. Nijhoff, F. Hartl, D.J. Stufkens, J.J. Piet, J.M. Warman, J. Chem. Soc., Chem. Commun. (1999) 991.
[89] J. Nijhoff, F. Hartl, J.W.M. van Outersterp, D.J. Stufkens, M.J. Calhorda, L.F. Veiros, J. Organomet. Chem. 573 (1999) 121.
[90] J. Nijhoff, F. Hartl, D.J. Stufkens, J. Fraange, Organometallics 18 (1999) 4380.
[91] A.J. Deeming, M.J. Stchedroff, C. Whittaker, A.J. Arce, Y. De Sanctis, J.W. Steed, J. Chem. Soc., Dalton Trans. (1999) 3289.
[92] P. Nombel, N. Lugan, B. Donnadieu, G. Lavigne, Organometallics 18 (1999) 187.
[93] S. Aime, M. Férriz, R. Gobetto, E. Valls, Organometallics 18 (1999) 2030.
[94] J. Akther, K.A. Azam, A.R. Das, M.B. Hursthouse, S.E. Kabir, K.M. Abdul Malik, E. Rosenberg, M. Tesmer, H. Vahrenkamp, J. Organomet. Chem. 588 (1999) 211.
[95] F.-S. Kong, W.-T. Wong, J. Organomet. Chem. 589 (1999) 180.
[96] V. Ferrand, A. Neels, H. Stoeckli-Evans, G. Süss-Fink, Inorg. Chem. Commun. 2 (1999) 561.
[97] L. Xu, Y. Sasaki, Inorg. Chem. Commun. 2 (1999) 121.
[98] S. Ali, A.J. Deeming, G. Hogarth, N.A. Mehta, J.W. Steed, J. Chem. Soc., Chem. Commun. (1999) 2541.
[99] J.S. McIndoe, B.K. Nicholson, J. Organomet. Chem. 573 (1999) 232.
[100] R. Smith, E. Rosenberg, K.I. Hardcastle, V. Vazquez, J. Roh, Organometallics 18 (1999) 3519.
[101] M. Shieh, J. Clust. Sci. 10 (1999) 3.
[102] S.N. Konchenko, A.V. Virovets, N.A. Pushkarevsky, Inorg. Chem. Commun. 2 (1999) 552.
[103] A. Shaver, M. El-Khateeb, A.-M. Lebuis, Inorg. Chem. 38 (1999) 5913.
[104] R.D. Adams, W. Huang, J. Organomet. Chem. 573 (1999) 14.
[105] R.D. Adams, J.L. Perrin, J. Organomet. Chem. 582 (1999) 9.
[106] R.D. Adams, O.-S. Kwon, J.L. Perrin, J. Organomet. Chem. 584 (1999) 223.
[107] A.J. Arce, A. Karam, Y. De Sanctis, M.V. Capparelli, A.J. Deeming, Inorg. Chim. Acta 285 (1999) 277.
[108] R. Dilshad, K.M. Hanif, M.B. Hursthouse, S.E. Kabir, K.M. Abdul Malik, E. Rosenberg, J. Organomet. Chem. 585 (1999) 100.
[109] K.M. Hanif, M.B. Hursthouse, S.E. Kabir, K.M. Abdul Malik, E. Rosenberg, J. Organomet. Chem. 580 (1999) 60.
[110] E.W. Ainscough, A.M. Brodie, R.K. Coll, J.M. Waters, Aust. J. Chem. 52 (1999) 801.
[111] R.W. Eveland, C.C. Raymond, T.E. Albrecht-Schmitt, D.F. Shriver, Inorg. Chem. 38 (1999) 1282.
[112] J. Huang, H.-J. Schanz, E.D. Stevens, S.P. Nolan, Organometallics 18 (1999) 2370.
[113] Q.D. Shelby, W. Lin, G.S. Girolami, Organometallics 18 (1999) 1904.
[114] H.-J. Jeon, N. Prokopuk, C. Stern, D.F. Shriver, Inorg. Chim. Acta 286 (1999) 142.
[115] H. Nagashima, A. Suzuki, H. Kondo, M. Nobata, K. Aoki, K. Itoh, J. Organomet. Chem. 580 (1999) 239.
[116] P. Frediani, A. Salvini, S. Finocchiaro, J. Organomet. Chem. 584 (1999) 265.
[117] C.S.-W. Lau, W.-T. Wong, J. Organomet. Chem. 588 (1999) 113.
[118] K.S.-Y. Leung, Y. Li, Inorg. Chem. Commun. 2 (1999) 599.
[119] W.-Y. Yeh, C.-Y. Wu, L.-W. Chiou, Organometallics 18 (1999) 3547.
[120] Y.-Y. Choi, W.-T. Wong, J. Organomet. Chem. 573 (1999) 189.
[121] M.I. Bruce, B.W. Skeleton, A.H. White, N.N. Zaitseva, Aust. J. Chem. 52 (1999) 681.
[122] H.G. Ang, S.G. Ang, S. Du, J. Chem. Soc., Dalton Trans. (1999) 2963.
[123] Y.-Y. Choi, W.-T. Wong, J. Chem. Soc., Dalton Trans. (1999) 331.
[124] M. Akita, A. Sakurai, Y. Moro-oka, J. Chem. Soc., Chem. Commun. (1999) 101.
[125] C.J. Adams, M.I. Bruce, B.W. Skelton, A.H. White, Aust. J. Chem. 52 (1999) 409.
[126] C.J. Adams, M.I. Bruce, B.W. Skelton, A.H. White, J. Organomet. Chem. 573 (1999) 134.
[127] C.J. Adams, M.I. Bruce, B.W. Skelton, A.H. White, J. Organomet. Chem. 584 (1999) 254.
[128] C.J. Adams, M.I. Bruce, B.W. Skelton, A.H. White, J. Chem. Soc., Dalton Trans. (1999) 1283.
[129] C.J. Adams, M.I. Bruce, B.W. Skelton, A.H. White, J. Chem. Soc., Dalton Trans. (1999) 2451.
[130] C.J. Adams, M.I. Bruce, B.W. Skelton, A.H. White, J. Organomet. Chem. 589 (1999) 213.
[131] W.J. Dollard, P.J. Dyson, T. Jackson, B.F.G. Johnson, J.S. McIndoe, P.R.R. Langridge-Smith, Inorg. Chem. Commun. 2 (1999) 587.

[132] D.H. Farrar, A.J. Poë, R. Ramachandran, J. Organomet. Chem. 573 (1999) 217.
[133] T. Chihara, T. Tase, H. Ogawa, Y. Wakatsuki, J. Chem. Soc., Chem. Commun. (1999) 279.
[134] P. Schooler, B.F.G. Johnson, S. Parsons, J. Chem. Soc., Dalton Trans. (1999) 559.
[135] P. Schooler, B.F.G. Johnson, L. Scaccianoce, R. Tregonning, J. Chem. Soc., Dalton Trans. (1999) 2743.
[136] K.S.-Y. Leung, W.-T. Wong, J. Chem. Soc., Dalton Trans. (1999) 2521.
[137] K.S.-Y. Leung, W.-T. Wong, J. Chem. Soc., Dalton Trans. (1999) 2077.
[138] K.S.-Y. Leung, W.-T. Wong, Eur. J. Inorg. Chem. (1999) 1757.
[139] K.S.-Y. Leung, Inorg. Chem. Commun. 2 (1999) 498.
[140] R. Tannenbaum, G. Bor, J. Organomet. Chem. 586 (1999) 18.
[141] H. Wadepohl, K. Büchner, M. Herrmann, H. Pritzkow, J. Organomet. Chem. 573 (1999) 22.
[142] J.D. King, M. Monari, E. Nordlander, J. Organomet. Chem. 573 (1999) 272.
[143] J. Zhang, X-N. Chen, Y.-Q. Yin, W.-L. Wang, X.-Y. Huang, J. Organomet. Chem. 582 (1999) 252.
[144] G. Conole, J.E. Davies, J.D. King, M.J. Mays, M. McPartlin, H.R. Powell, P.R. Raithby, J. Organomet. Chem. 585 (1999) 141.
[145] J.L. Kerr, B.H. Robinson, J. Simpson, J. Chem. Soc., Dalton Trans. (1999) 4165.
[146] P.A. Brooksby, N.W. Duffy, A.J. McQuillan, B.H. Robinson, J. Simpson, J. Organomet. Chem. 582 (1999) 183.
[147] V. Calvo-Perez, M. Shang, G.P.A. Yap, A.L. Rheingold, T.P. Fehlner, Polyhedron 18 (1999) 1869.
[148] S.G. Bott, J.C. Wang, M.G. Richmond, J. Chem. Crystallogr. 29 (1999) 603.
[149] M.P. Castellani, W.G. Smith, N.G. Patel, S.G. Bott, M.G. Richmond, J. Chem. Crystallogr. 29 (1999) 609.
[150] T. Iwasa, H. Shimada, A. Takami, H. Matsuzaka, Y. Ishii, M. Hidai, Inorg. Chem. 38 (1999) 2851.
[151] T. Eguchi, B.T. Heaton, J. Chem. Soc., Dalton Trans. (1999) 3523.
[152] L.J. Farrugia, D. Braga, F. Grepioni, J. Organomet. Chem. 573 (1999) 60.
[153] P. Macchi, L. Garlaschelli, S. Martinengo, A. Sironi, J. Am. Chem. Soc. 121 (1999) 10428.
[154] X.-N. Chen, J. Zhang, S.-L. Wu, Y.-Q. Yin, W.-L. Wang, J. Sun, J. Chem. Soc., Dalton Trans. (1999) 1987.
[155] F.-E. Hong, Y.-C. Chang, R.-E. Chang, C.-C. Lin, S.-L. Wang, F.-L. Liao, J. Organomet. Chem. 588 (1999) 160.
[156] I. Matsuda, Y. Fukuta, K. Itoh, Inorg. Chim. Acta 296 (1999) 72.
[157] J. Feng, M. Garland, Organometallics 18 (1999) 417.
[158] J. Feng, M. Garland, Organometallics 18 (1999) 1542.
[159] M.A. Casado, J.J. Pérez-Torrente, J.A. López, M.A. Ciriano, F.J. Lahoz, L.A. Oro, Inorg. Chem. 38 (1999) 2482.
[160] T. Kochi, Y. Tanabe, Z. Tang, Y. Ishii, M. Hidai, Chem. Lett. (1999) 1279.
[161] S.M. Contakes, M. Schmidt, T.B. Rauchfuss, J. Chem. Soc., Chem. Commun. (1999) 1183.
[162] J. Chen, R.J. Angelici, Organometallics 18 (1999) 5721.
[163] X. Lei, M. Shang, T.P. Fehlner, J. Chem. Soc., Chem. Commun. (1999) 933.
[164] S.-W. Zhang, T. Kaneko, E. Yoneda, T. Sugioka, S. Takahashi, Inorg. Chim. Acta 296 (1999) 195.
[165] R.D. Pergola, L. Garlaschelli, M. Mannassero, M. Sansoni, J. Clust. Sci. 10 (1999) 109.
[166] A. Fukuoka, M. Osada, T. Shido, S. Inagaki, Y. Fukushima, M. Ichikawa, Inorg. Chim. Acta 294 (1999) 281.
[167] T. Tanase, M. Hamaguchi, R.A. Begum, S. Yano, Y. Yamamoto, J. Chem. Soc., Chem. Commun. (1999) 745.
[168] S. Arifhodzic-Radojevic, A.D. Burrows, N. Choi, M. McPartlin, D.M.P. Mingos, S.V. Tarlton, R. Vilar, J. Chem. Soc., Dalton Trans. (1999) 3981.
[169] J.R. Berenguer, E. Equizàbal, L.R. Falvello, J. Forniés, E. Lalinde, A. Martín, Organometallics 18 (1999) 1653.
[170] S.V. Tarlton, N. Choi, M. McPartlin, D.M.P. Mingos, R. Vilar, J. Chem. Soc., Dalton Trans. (1999) 653.

[171] J.V. Barkley, T. Eguchi, R.A. Harding, B.T. Heaton, G. Longoni, L. Manzi, H. Nakayama, K. Miyagi, A.K. Smith, A. Steiner, J. Organomet. Chem. 573 (1999) 254.
[172] A. Ceriotti, N. Masciocchi, P. Macchi, G. Longoni, Angew. Chem., Int. Ed. 38 (1999) 3724.
[173] F. Calderoni, F. Demartin, F.F. de Biani, C. Femoni, M.C. Iapalucci, G. Longoni, P. Zanello, Eur. J. Inorg. Chem. (1999) 663.
[174] F. Demartin, C. Femoni, M.C. Iapalucci, G. Longoni, P. Macchi, Angew. Chem., Int. Ed. 38 (1999) 531.
[175] V.W.-W. Yam, W.K.-M. Fung, K.-K. Cheung, J. Clust. Sci. 10 (1999) 37.
[176] K.A. Al-Farhan, M.H. Ja'far, O.M. Abu-Salah, J. Organomet. Chem. 579 (1999) 59.
[177] V.W.-W. Yam, K.K.-W. Lo, K.M.-C. Wong, J. Organomet. Chem. 578 (1999) 3.
[178] J.E. Casas, M.C. Gimeno, P.G. Jones, A. Laguna, M. Laguna, J. Chem. Soc., Dalton Trans. (1999) 2819.
[179] M.A. Casado, J.J. Pérez-Torrente, M.A. Ciriano, A.J. Edwards, F.J. Lahoz, L.A. Oro, Organometallics 18 (1999) 5299.
[180] M. Nihei, T. Nankawa, M. Kurihara, H. Nishihara, Angew. Chem., Int. Ed. 38 (1999) 1098.
[181] K. Kuge, H. Tobita, H. Ogino, J. Chem. Soc., Chem. Commun. (1999) 1061.
[182] L.-C. Song, Y.-B. Dong, Q.-M. Hu, W.-Q. Gao, D.-S. Guo, P.-C. Liu, X.-Y. Huang, J. Sun, Organometallics 18 (1999) 2168.
[183] F. Xu, S.Y. Yang, W.H. Sun, J.Y. Yu, K.B. Yu, Polyhedron 18 (1999) 1541.
[184] J.-P. Lang, K. Tatsumi, J. Organomet. Chem. 579 (1999) 332.
[185] H. Brunner, D. Mijolovic, B. Wrackmayer, B. Nuber, J. Organomet. Chem. 579 (1999) 298.
[186] K.K.-H. Lee, W.-T. Wong, J. Organomet. Chem. 577 (1999) 323.
[187] M. Yuki, M. Okazaki, S. Inomata, H. Ogino, Organometallics 18 (1999) 3728.
[188] M.E. García, V. Riera, M.T. Rueda, M.A. Ruiz, M. Lanfranchi, A. Tiripicchio, J. Am. Chem. Soc. 121 (1999) 4060.
[189] P. Braunstein, U. Englert, G.E. Herberich, M. Neuschütz, M.U. Schmidt, J. Chem. Soc., Dalton Trans. (1999) 2807.
[190] W.-F. Liaw, C.-M. Lee, L. Horng, G.-H. Lee, S.-M. Peng, Organometallics 18 (1999) 782.
[191] A.B. Antonova, A.A. Johansson, N.A. Deykhina, D.A. Pogrebnyakov, N.I. Pavlenko, A.I. Rubaylo, F.M. Dolgushin, P.V. Petrovskii, A.G. Ginzburg, J. Organomet. Chem. 577 (1999) 238.
[192] K. Panneerselvam, T.-H. Lu, S.-F. Tung, A.K. Dash, P. Mathur, Acta Cryst. C55 (1999) 1250.
[193] A.R. Manning, L. O'Dwyer, P.A. McArdle, D. Cunningham, J. Organomet. Chem. 573 (1999) 109.
[194] W.H. Watson, A. Nagl, M.-J. Don, M.G. Richmond, J. Chem. Crystallogr. 29 (1999) 871.
[195] S.G. Bott, J.C. Wang, H. Shen, M.G. Richmond, J. Chem. Crystallogr. 29 (1999) 391.
[196] S. Bouherour, P. Braunstein, J. Rosé, L. Toupet, Organometallics 18 (1999) 4908.
[197] P.J. Low, R. Rousseau, P. Lam, K.A. Udachin, G.D. Enright, J.S. Tse, D.D.M. Wayner, A.J. Carty, Organometallics 18 (1999) 3885.
[198] X.-N. Chen, J. Zhang, Y.-Q. Yin, W.-L. Wang, Chem. Lett. (1999) 583.
[199] T. Kochi, Y. Nomura, Z. Tang, Y. Ishii, Y. Mizobe, M. Hidai, J. Chem. Soc., Dalton Trans. (1999) 2575.
[200] B.T. Sterenberg, M.C. Jennings, R.J. Puddephatt, Organometallics 18 (1999) 2162.
[201] M. Benito, O. Rossell, M. Seco, G. Segalés, Organometallics 18 (1999) 5191.
[202] H. Wadepohl, S. Gebert, R. Merkel, H. Prizkow, J. Chem. Soc., Chem. Commun. (1999) 389.
[203] I. Bachert, I. Bartusseck, P. Braunstein, E. Guillon, J. Rosé, G. Kickelbick, J. Organomet. Chem. 580 (1999) 257.
[204] B.T. Sterenberg, H.A. Jenkins, R.J. Puddephatt, Organometallics 18 (1999) 219.
[205] L.R. Falvello, S. Fernàndez, R. Navarro, E.P. Urriolabeitia, Inorg. Chem. 38 (1999) 2455.
[206] T. Amemiya, S. Kuwata, M. Hidai, J. Chem. Soc., Chem. Commun. (1999) 711.
[207] M.A. Casado, M.A. Ciriano, A.J. Edwards, F.J. Lahoz, L.A. Oro, J.J. Pérez-Torrente, Organometallics 18 (1999) 3025.
[208] M.A. Casado, J.J. Pérez-Torrente, M.A. Ciriano, L.A. Oro, A. Orejón, C. Claver, Organometallics 18 (1999) 3035.

[209] M. Yuki, K. Kuge, M. Okazaki, T. Mitsui, S. Inomata, H. Tobita, H. Ogino, Inorg. Chim. Acta 291 (1999) 395.
[210] K.V. Adams, N. Choi, G. Conole, J.E. Davies, J.D. King, M.J. Mays, M. McPartlin, P.R. Raithby, J. Chem. Soc., Dalton Trans. (1999) 3679.
[211] L. Plasseraud, H. Stoeckli-Evans, G. Süss-Fink, Inorg. Chem. Commun. 2 (1999) 344.
[212] P. Mathur, S. Chatterjee, S. Ghose, M.F. Mahon, J. Organomet. Chem. 587 (1999) 93.
[213] S.M. Waterman, M.G. Humphrey, D.C.R. Hockless, J. Organomet. Chem. 582 (1999) 310.
[214] J. Zhang, X.-N. Chen, Y.-Q. Yin, X.-Y. Huang, J. Organomet. Chem. 579 (1999) 304.
[215] C.E. Housecroft, D.M. Nixon, A.L. Rheingold, Polyhedron 18 (1999) 2415.
[216] S.M. Waterman, M.G. Humphrey, Organometallics 18 (1999) 3116.
[217] S.M. Waterman, M.G. Humphrey, J. Lee, G.E. Ball, D.C.R. Hockless, Organometallics 18 (1999) 2440.
[218] S.M. Waterman, M.G. Humphrey, J. Lee, J. Organomet. Chem. 589 (1999) 226.
[219] T.-K. Huang, Y. Chi, S.-M. Peng, G.-H. Lee, Organometallics 18 (1999) 1675.
[220] U. Brand, C.A. Wright, J.R. Shapley, Inorg. Chem. 38 (1999) 5910.
[221] S. Ghosh, M. Shang, T.P. Fehlner, J. Am. Chem. Soc. 121 (1999) 7451.
[222] Y. Chi, C. Chung, W.-C. Tseng, Y.-C. Chou, S.-M. Peng, G.-H. Lee, J. Organomet. Chem. 574 (1999) 294.
[223] S.M. Waterman, M.G. Humphrey, D.C.R. Hockless, J. Organomet. Chem. 579 (1999) 75.
[224] V.G. Albano, C. Castellari, C. Femoni, M.C. Iapalucci, G. Longoni, M. Monari, M. Rauccio, S. Zacchini, Inorg. Chim. Acta 291 (1999) 372.
[225] M.I. Bruce, N.N. Zaitseva, B.W. Skelton, A.H. White, J. Chem. Soc., Dalton Trans. (1999) 2777.
[226] S. Haak, A. Neels, H. Stoeckli-Evans, G. Süss-Fink, C.M. Thomas, J. Chem. Soc., Chem. Commun. (1999) 1959.
[227] V. Ferrand, G. Süss-Fink, A. Neels, H. Stoeckli-Evans, Eur. J. Inorg. Chem. 2 (1999) 853.
[228] A.U. Härkönen, M. Ahlgrén, T.A. Pakkanen, J. Pursiainen, J. Organomet. Chem. 573 (1999) 225.
[229] G. Süss-Fink, S. Haak, V. Ferrand, H. Stoeckli-Evans, J. Mol. Catal. A: Chem. 143 (1999) 163.
[230] W.-T. Wong, Organometallics 18 (1999) 3474.
[231] G. Süss-Fink, S. Haak, V. Ferrand, A. Neels, H. Stoeckli-Evans, J. Organomet. Chem. 580 (1999) 225.
[232] S.Y.-W. Hung, W.-T. Wong, J. Organomet. Chem. 580 (1999) 48.
[233] F.-S. Kong, W.T. Wong, J. Chem. Soc., Dalton Trans. (1999) 2497.
[234] V.G. Albano, C. Castellari, M.C. Iapalucci, G. Longoni, M. Monari, A. Paselli, S. Zacchini, J. Organomet. Chem. 573 (1999) 261.
[235] F.M. Dolgushin, E.V. Grachova, B.T. Heaton, J.A. Iggo, I.O. Koshevoy, I.S. Podkorytov, D.J. Smawfield, S.P. Tunik, R. Whyman, A.I. Yanovskii, J. Chem. Soc., Dalton Trans. (1999) 1609.
[236] J.H. Yamamoto, G.D. Enright, A.J. Carty, J. Organomet. Chem. 577 (1999) 126.
[237] P. Mathur, M.O. Ahmed, A.K. Dash, M.G. Walawalkar, J. Chem. Soc., Dalton Trans. (1999) 1795.
[238] M. Yuki, M. Okazaki, H. Ogino, Chem. Lett. (1999) 649.
[239] W. Clegg, N. Feeder, A.M.M. Castro, S. Nahar, P.R. Raithby, G.P. Shields, S.J. Teat, J. Organomet. Chem. 573 (1999) 237.
[240] N.L. Cromhout, J.F. Gallagher, J. Lewis, P.R. Raithby, Inorg. Chem. Commun. 2 (1999) 389.
[241] S. Haak, A. Neels, H. Stoeckli-Evans, G. Süss-Fink, Inorg. Chem. Commun. 2 (1999) 60.
[242] M.I. Bruce, J.-F. Halet, S. Kahlal, P.J. Low, B.W. Skelton, A.H. White, J. Organomet. Chem. 578 (1999) 155.
[243] Y. Katsukawa, S. Onaka, Y. Yamada, M. Yamashita, Inorg. Chim. Acta 294 (1999) 255.
[244] R.D. Adams, U.H.F. Bunz, W. Fu, L. Kloppenburg, B. Qu, Inorg. Chem. Commun. 2 (1999) 1.
[245] J.W.-S. Hui, W.-T. Wong, J. Clust. Sci. 10 (1999) 91.
[246] M. Stener, K. Albert, N. Rösch, Inorg. Chim. Acta 286 (1999) 30.
[247] M.-C. Chung, A. Sakurai, M. Akita, Y. Moro-oka, Organometallics 18 (1999) 4684.
[248] H.-G. Ang, S.-G. Ang, S. Du, J. Organomet. Chem. 589 (1999) 133.
[249] A.J. Amoroso, M.A. Beswick, C.-K. Li, J. Lewis, P.R. Raithby, M.C.R. de Arellano, J. Organomet. Chem. 573 (1999) 247.

[250] M.I. Bruce, B.W. Skelton, A.H. White, N.N. Zaitseva, Inorg. Chem. Commun. 2 (1999) 453.
[251] J.-P. Lang, K. Tatsumi, Inorg. Chem. 38 (1999) 1364.
[252] I. Ara, J. Gómez, E. Lalinde, R.I. Merino, M.T. Moreno, Inorg. Chem. Commun. 2 (1999) 62.
[253] M. Benito, O. Rossell, M. Seco, G. Segalés, Inorg. Chim. Acta 291 (1999) 247.
[254] J.P.H. Charmant, J. Forniés, J. Gómez, E. Lalinde, R.I. Merino, M.T. Moreno, A.G. Orpen, Organometallics 18 (1999) 3353.
[255] N.T. Tran, M. Kawano, D.R. Powell, R.K. Hayashi, C.F. Campana, L.F. Dahl, J. Am. Chem. Soc. 121 (1999) 5945.